Summer 1998

Effect of Pulsed Electric Fields on Aquatic Nuisance Species

Amr Abou-Ghazala
Old Dominion University

EFFECT OF PULSED ELECTRIC FIELDS ON AQUATIC NUISANCE SPECIES

by

Amr Abou-Ghazala
B.Sc. June 1990, University of Alexandria, Egypt
M.Sc. March 1994 University of Alexandria, Egypt

A Dissertation Submitted to the Faculty of
Old Dominion University in Partial Fulfillment of the
Requirement for the Degree of

DOCTOR OF PHILOSOPHY

ELECTRICAL ENGINEERING

OLD DOMINION UNIVERSITY
August 1998

Approved by:

_____

_____
Vishnu K. Lakdawala (Member)

_____
Linda L. Vahala (Member)

_____
Fred C. Dobbs (Member)

ABSTRACT

EFFECT OF PULSED ELECTRIC FIELDS ON AQUATIC NUISANCE SPECIES.

Amr Abou-Ghazala
Old Dominion University, 1998
Director: Dr. Karl H. Schoenbach

Clinical and theoretical evidence indicate that electric fields have biological effects ranging from recoverable disturbance to mortality induction depending on the field parameters and time of exposure. In this thesis, the effect of electrical field in pulsed form on aquatic nuisance species is investigated. Pulse parameters in terms of amplitude, width, shape, and repetition rate that stimulate the species to desirable levels are to be defined. Applying the electrical pulses with appropriate parameters to stun aquatic nuisance species entering marine cooling systems will prevent it from attaching to pipe walls. The use of electrical fields to seek efficient, environmentally friendly, and inexpensive solution for the biofouling problem is studied.

Laboratory experiments were performed on a "representative" species, the hydrozoan *Stylactis arge,* to achieve parameter optimization. In these experiments, four pulse generators were used to generate electric field strength of 100 V/cm to 20 kV/cm, with pulse width of 300 ns to 15 μs. Two field experiments were constructed to validate the idea of using the electric field in biofouling prevention.

Laboratory experiments showed that a combination of electric field strength and energy density is the crucial factor that determines the stunning

duration. It was found that a sub-lethal pulse could be effective if repeated. Repetition rate was shown to be an important parameter to gain cumulative effects of successive pulses. It was also concluded that semiconductor technology can not provide simple pulsers for the application of biofouling prevention; rather, gas tube or magnetic switches should be used for large field systems. Field experiments confirmed the laboratory observations. Electric fields of 12 kV/cm and 6.45 kV/cm at pulse width of 770 ns were able to prevent biofouling in salt water with an efficiency of 100% with a consumption of 1200 Gal/kWh. The fresh water trial, currently running, showed a promising start.

ACKNOWLEDGEMENTS

It has been a great pleasure to work with and learn from Dr. Karl Schoenbach. The inspiration for this work was his, and he kept it going with dedication and enthusiasm. I can not thank him enough for his continuous support and guidance; I would not have gone so far without him.

I would like to thank Ray Alden and Ted Turner for their contribution to this thesis. Dr. Alden introduced me to the world of aquatic species, and generously provided me the use of his laboratory. His suggestions resulted in clear improvements to this work. Ted Turner provided useful practical experience in dealing with these species. Their encouragement is also appreciated.

The sponsors of biofouling prevention projects have done more than simply provide the funds. Their interest and support have provided me many opportunities to meet and discuss my work with others in the Navy and power plant communities and gain field experience. I gratefully acknowledge the support of CASRM, Inc., Tennessee Valley Authority, Ontario Hydro, Rochester Gas and Electric, USAEWES, and ENTERGY. I would specially like to thank Thomas Fox of CASRM, Inc. and Garry Smythe of Acres International, who coordinated the field projects, Mr. Smythe also served as the external reviewer.

I would like to thank the members of my exam committee, Fred Dobbs, Vishnu Lakdawala, Linda Vahala. Their support allowed me to progress rapidly with my research and their encouragement is greatly appreciated.

Ray Allen deserves many thanks for getting me out of so many scraps.

TABLE OF CONTENTS

LIST OF TABLES

LIST OF FIGURES

FIGURE Page

CHAPTER I

INTRODUCTION

1.1 Background

Aquatic nuisance species are those water living organisms that hinder the performance of marine systems. They number in thousands ranging from primitive species (e.g. jellyfish) to more advanced, bone-fish species (e.g. ruffe). Some species native to the area, others are non-indigenous. Transportation mechanisms for these species vary from natural ways to man assisted ways. In most cases these organisms cause efficiency degradation to marine systems by many ways including attaching to hard surfaces and clogging water flow pipes.

The introduction of non-indigenous aquatic species throughout North America, for example, has been diversified. The Atlantic coast has been populated with nuisance species of hydroids, barnacles, water fleas, crabs, shrimps, and mussels. Nonnative sea squirts, diatoms, and worms have been discovered from the shores of the Canadian Maritime Provinces down to the state of Florida. Areas such as the Chesapeake Bay, or Hudson River are substantially affected by these introductions. Ports such as New York, Norfolk, and Newport News teem with life, much of it very different from what once existed.

Dispersal mechanisms for these species include ship hulls and ballast water exchange. The most common form of inadvertent transfer of any species was on the hulls of a wooden sailing ships. Large quantities of living marine material collected from all over the world usually foul the bottom of sailing ships. These ships were usually careened on the shore to scrap off masses of

---

Journal model used for this dissertation is *Proceedings of the IEEE*.

seaweed, hydroids, sea squirts, and bacteria. As a result these organisms were deposited many thousands of miles from their origin. Ballast water also is blamed for the transfer of aquatic nuisance species. This water tanks which provide stability to the ships usually contain species belonging to the harbor from which it was taken. When this water is discharged at the final destination, the organisms are released into the receiving water, resulting in a potential new invasion.

The aquatic nuisance species problem has significant economic and ecological implications. The clogging of pipes due to biofouling organisms capable of rapid population growth is a major problem in cooling systems where untreated lake, river, or seawater is used. In estuarine and marine ecosystems it is blue mussels and barnacles, in freshwater ecosystems zebra and quagga mussels, whose uncontrolled growth causes problems. These organisms are often drawn into the cooling system where they may become attached and reproduce very rapidly. This affects water flow and thus reducing the cooling efficiency, in general, and can present an increased potential hazard on nuclear powered vessels. Figure 1 shows an example of a biofouling problem in water pipes, where zebra mussels clogged a 2-inch pipe only 14 days after chlorination. Attachment to ship hulls is another major problem of biofouling species. They increase water resistance and thus decrease fuel efficiency and maximum ship velocity. Millions of dollars are spent each year to remove attachments of these species from ship hulls. Down time is also a precious price paid for getting rid of fouling organisms. The economic impacts of some species are particularly large. The long-term impact of zebra mussels, for example, has been calculated in the billions of dollars [10].

(from Sea Grant Web site with permission)

Fig. 1. Fouling of pipes by aquatic species

1.2 Current Solutions to the Biofouling Problem

The problem of biofouling was noted as early as the fifth century BC [6]. Since then, efforts have been conducted to find economical and efficient solutions. Development of antifouling solutions during the nineteenth century appears to be guided only by practical experience. Devices for removing fouling, that include various systems of chains or knives for scrapping the ships' bottom, were common solutions. In the beginning of the twentieth century more scientific solutions were used, such as antifouling paints and electrical solutions. Recently, the fouling problem has been subjected to scientific inquiry because of its increased severity and the increased public concern to environmentally friendly solutions. Current methods to prevent biofouling or to remove biofoulants can be divided into chemical methods and non-chemical methods.

Chemical control methods that are currently being implemented include use of chlorine, chlorine dioxide, potassium permanganate, and ozonization. Advantages and disadvantages of chemical treatments have been debated for a long time and there is continuous research in this area to reach an optimum solution. Chlorine compounds have generally proved affordable and effective solutions to prevent biofouling. Consequently, they are widely used in the water supply industry and nuclear power plants. However, chlorine and chlorine derived products contribute to total trihalomethane production (TTHM). Present maximum allowable level for TTHM in the United States is one hundred parts per billion as established by the Environmental Protection Agency (EPA) and lower levels are to be enforced in few years [5]. This will profoundly limit the use of chlorine and

its derivatives as a biofouling control method. Potassium permanganate ($KMnO_4$) is a relatively recent suggestion to avoid TTHM introduction to the environment. To date, its use by water treatment systems primarily has been for taste and odor control. However, research is on the way to optimize its dosage and investigate its efficiency as a biofouling control method. Ozonization has proven to be an effective, environmentally friendly solution. However, a high concentration is needed, 0.2 mg/liter [17], to obtain satisfactory results; moreover, due to the short half-life of ozone, a large number of highly concentrated injections are needed along the water line. This makes ozonization economically unfeasible.

Non-chemical control methods can be sub-divided into non-electrical methods and electrical methods. Non-electrical methods include mechanical scraping, pigging, thermal treatment, and use of paint or other coatings. Mechanical scraping is physical removing of foulants either by hand tools or advanced machinery. High-pressure spray washing is often used as an alternative to scraping. The pigging process involves the forcing of chemical substance like soft polyethylene through the water line using water pressure, thus removing deposits from the inner wall of the pipes. The disadvantages of these methods are the need of extensive effort and consumption of time. Heat is effective; high temperatures, 104°F and above, have been shown to kill zebra mussels almost instantaneously [23]. It also dissipates rapidly, leaving no chemical pollutants or bi-products. The difficulties in the use of heat involve the application of the heat to the locations of the organisms, which in most cases is in either a running flow or a very vast area; using heat in cooling systems also

has functional limitations. However, any of the above scraping methods should be applied prior to the application of any other preventive solution. Toxic paint solution was introduced in 1860 by J. McIness [6]. Toxic paint, after being modified many times from its original mixture, proved to be efficient. The effective coatings act by poisoning the organisms at the time of attachment or shortly after. But still the release of toxic compounds, like copper sulfate, into the environment is its main disadvantage. Moreover, the paint needs to be reapplied after a few years. This may be due to loss of adhesion to conduit walls or because the toxic material has ablated out of the paint, or epoxy. The life of a toxic paint is determined by the thickness of the coating, and its rate of dissolution. Difficulty in applying these paints to the inside of cooling system pipes is another restriction to these paints.

Electrical control methods to prevent biofouling have a rich history in USA and in Europe. Patents as old as 1863 claim the use of electricity for protecting a ship's bottom from fouling and corrosion [24]. In 1891, Thomas Edison was granted a patent for an electric antifouling system having a DC generator on the ship, which fed multiple electric cables with electrodes at their ends in order to send electric currents back through the ship's hull to prevent the attachment of organisms [6]. Several patents were claimed later using the concept of electrical biofouling prevention but with different strategy and setups [i.e., 25,26,27]. However, most of these patents have never been tested seriously due to both the complexity of the problem and the acceptance of the inexpensive chemical, environmentally hazardous solutions.

Recently, the problem of biofouling became more severe and gained public attention. Invasions of new organisms capable of rapid growth and with no natural predators, i.e. zebra mussels and ruffe, have increased the seriousness of the problem and gained the attention of related industries who have the potential to loose millions each year if fouled or in developing their prevention program. Consequently, practical solutions were sought taking into account the environmental regulations imposed by different state and federal agencies. Electrical methods can bridge this gap between environmental acceptability and effective control. Different electrical strategies were tried recently with seemingly conflicting results. These methods include acoustic, ultrasonic, gamma radiation, UV radiation and electrical fields. Acoustic methods refer to pulsed acoustic generation by electric discharge in water. Reported results of these methods range from negative [11] to positive [17]. Ultrasonic, above the audible band, refers to the launching of underwater sinusoidal pressure waves from continuous wave generators in the frequency range of a few hundred hertz to 1 megahertz. UV was proposed to prevent the settling of some organisms that do not have protective structures like shells. Expensive installation, and high power requirements limit the use of this technique.

It is well known that electric fields have an effect on biological systems. Effects range from stunning to killing biological organisms using the suitable field parameters. The idea of using this effect fit well for the application of biofouling control. DC and AC field trials were reported with promising results. It has been shown experimentally that electric fields on the order of 1 kV/cm will kill zebra

mussels in the free floating and adult stage [14]. In this field test, a continuous AC was used. However, if we extrapolate the electric fields required across a standard intake pipe it would require a small power plant to run in the steady state. In a more recent study [21], the use of capacitive discharge electric fields of 26 volts per centimeter (maximum) to deter attachment of zebra mussel showed promising results. New York State Electric and Gas Corporation conducted limited testing of high intensity electric barriers at their Kintigh Station in 1990 [5]. Zebra mussel mortality of 30% was reported for fields of 600 V/cm for 0.1 second duration. Based on calculations, the power requirement to effectively operate high intensity barriers at the station made this system impractical. Consequently, the use of pulsed power technology, i.e., short pulse generation up to a microsecond long with long gaps in between, is a logical alternative. The shorter the time of exposure, the larger the necessary electric field, but this effect is nonlinear as reported in many texts [15,17]. Maximum efficiency of this method is obtained by applying pulses in the microsecond range [17]. Using pulsed electric fields can therefore save energy and make the process more efficient and environmentally friendly. Advantages of pulsed power technology as a control method to biofouling problem include:

1) No chemicals are used or generated in any form.
2) Where the effort is to stun the mussels, there is no clean up of any kind needed.
3) Higher efficiency is obtained when the desired effect is dependent on peak power not on average energy.

4) Pulsed power allows processing in a time frame short enough to prevent thermal effects.

5) It is possible to stun or kill the biofoulants by tuning the power.

Pulsed electric fields were first tried by Russian scientists [5] who discharged a pulsed capacitor to create electric fields in the range of 600 to 3000 volts per centimeter and pulsed discharge times of 25 microseconds to125 microseconds. They applied the field to *Daphnia*. Stunning times up to 1000 seconds were reported. A more recent study [12] exposed mussels to pulsed electric fields with the objective of inhibiting mussel attachment during and after exposure to pulsed electric fields. The electric field was in the range of 16 volts per centimeter with rectangular pulses of width 0.5 millisecond. Significant settlement reduction (83-88%) on the treatment plates compared with control plates was reported.

1.3 Motivation

The aim of this research is to study the effect of short pulsed electric field on aquatic nuisance species, and optimize the field parameters in order to control species behavior. Effect of pulse shape, amplitude, repetition rate, and frequency spectrum on species response are studied. Hydrozoans (*Stylactis arge*), barnacles, living in tidal water, and zebra mussels living in fresh water were chosen for this study due to their high capacity for biofouling. Short-term effects, stunning period and instant mortality, and long-term effects, the ability to feed and late mortality, of pulsed electric fields on the hydrozoan were investigated via laboratory experiments. The feasibility of using pulsed electric field as an

efficient, environmentally friendly, and inexpensive control method to the biofouling problem in water flow systems was also investigated via field experiments in both salt water and fresh water.

CHAPTER II

EFFECT OF ELECTRIC FIELDS ON BIOLOGICAL CELLS

2.1 Biological Background

The basic unit of a living tissue is the cell. Cells can be grouped into two major types. Prokaryotic cells are simple in their structure, small in size (0.5-2 μm length), and lack a nucleus. All bacteria belong to this type. On the other hand, eukaryotic cells are much larger (from a few μm up to 100 μm length), and have internal membranes around a nucleus, and thicker walls. Organisms other than bacteria are all composed of one or more eukaryotic cells.

Cells are specialized in their anatomy and physiology to perform different tasks. Some organisms are composed of a single cell and others of trillions of cells. All cells have the same basic architecture; different broad classes of cells share this basic structure, however, the general plan is modified in various ways to meet various functions. A typical cell is composed of three elements:

1. A very thin, about 10nm, double layer of lipid, called the plasma membrane envelops the cell. This membrane isolates the cell from the outside world. The only connections between the cell and the outside world are through many pathways and communication channels that cross this membrane.
2. The nuclear region directs the activities of the cell. In bacteria the genetic material is included in a single circular molecule of DNA, unbounded by membranes.
3. A semifluid matrix called the cytoplasm occupies the volume between the nuclear region and the cell membrane. This semifluid cytoplasm contains the

chemical wealth of the cell including sugars, amino acids and proteins with which the cell carries out its everyday activities of growth and reproduction.

The cell membrane plays an important role in establishing the resting and active electric properties of an excitable cell, through its regulation of the movement of ions between the extracellular and intracellular spaces. The ease with which an ion crosses the membrane, namely the membrane permeability, differs among ion species. This selective permeability is altered as a result of the cell activation. Another important consideration for transmembrane ion movement is the fact that the ionic composition inside the cell differs greatly from that outside of the cell. Consequently, concentration gradients exist for all permeable ions that contribute to the net ion movement. Obeying diffusion principles, ions tends to accumulate at the inner and outer membrane surfaces, a process by which an electric field is established within the membrane. This field exerts forces on the ions crossing the membrane. This imbalance is accounted for by an active transport through ion pumps, e.g., the sodium- potassium pump, at the expense of metabolic energy. It is the presence of these concentration gradients, together with the difference in permeability of the membrane to these ions, that accounts for the resting membrane potential. In this resting state, the potential remains constant. All passive forces are exactly balanced by active forces. A steady state exists, even though there is still a strong concentration gradient of both K^+ and Na^+ in opposite directions, and there is a slight excess of positive charges in the extracellular space accompanied by a corresponding slight excess of negative charges in the intracellular space (enough to account

for a potential of the magnitude of 70 mV). At this point, although movement across the membrane is taking place by means of passive leaks and active pumping, the exchange of charges between the intracellular and extracellular are exactly balanced, with the potential that has been established by these forces remaining constant. Consequently, the resting state is not a passive state, but a stable active state that needs metabolic energy to be maintained [3].

2.2 Electrical Equivalent Circuit for Biological Cells

The existence of a connection between electrical phenomena and biological systems was discovered very early. Attempts to model biological cells and their components have been made in order to understand, analyze and communicate especially in educational research. Hodgkin and Huxley were the first to introduce a model that described the electrical behavior of the membrane, and won Nobel Prize for their contribution. This membrane model is shown in figure 2. According to this model, the current can be carried through the membrane by either charging the membrane capacitance or movement of different ions through the resistance that represents movement across the ionic channels. The ionic current consists of potassium and sodium ion currents and a small leakage current representing the chlorine and other ions. Each ionic current is derived by a driving force represented as a voltage source. The conductance of the membrane to different ion currents is a function of time and membrane potential.

A cell equivalent circuit of physical significance was developed by Schwan [23], and is shown in figure 3. It consists of a parallel combination of a series and

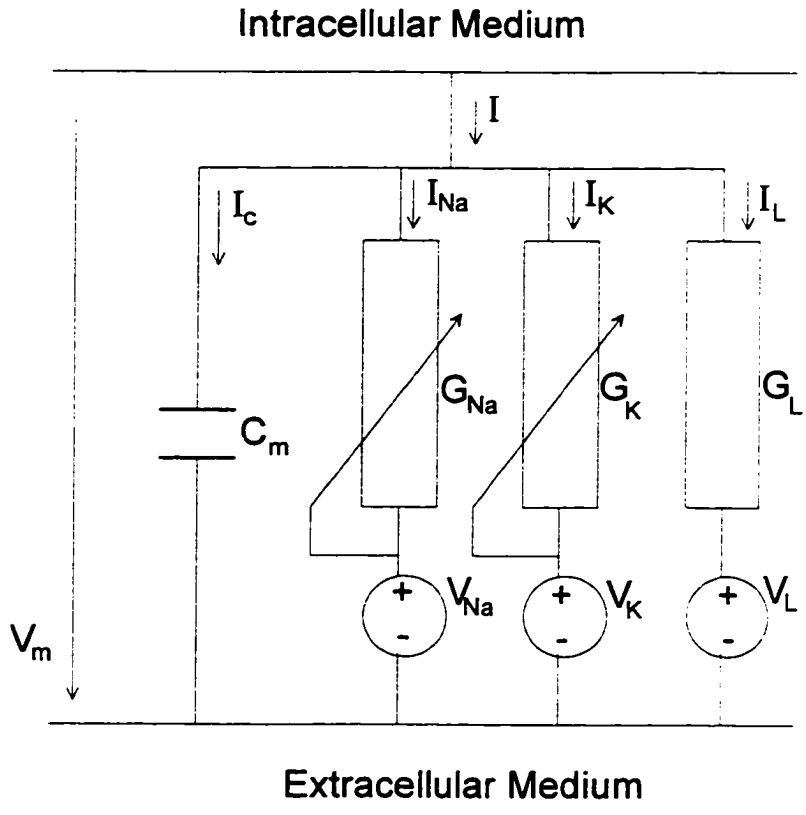

Fig. 2. Cellular membrane model as developed by Hodgkin and Huxley

a parallel RC combination. The parallel branch represents the dielectric constant and conductivity of the path that conducts electricity shunting the cell in the suspending medium. The series branch consists of a capacitance representing the membrane capacity and a resistance representing the cytoplasm; this branch determines the part of the current entering the cell. The objective of this model was to demonstrate that the cell interior is subjected to higher currents in the radio frequency range than low frequencies.

Based on the above models for the membrane and the cell, an electrical equivalent circuit of the cell in a suspension was derived to predict the cell behavior to the stimulating pulses [20]. The effect of membrane capacitance was taken into consideration for currents entering and leaving the cell, and the charging time constant for this model was calculated. The model of the cell, shown in figure 4, consists of resistors and capacitors for which values should be assigned based on size, shape, and known parameters. Eukaryotic cells vary in size from 2 μm to 100 μm, and different species have different natural suspension characteristics, therefore, the circuit parameter values are different from one species to another.

The cell immersed in the suspension is described by a capacitance C_m, the capacitance of the cell membrane, in series with the resistance of the cell interior, R_c. Typical capacitance values for the cell membranes are approximately 1 $\mu F/cm^2$ [13]. The cell interior has a resistivity on the order of 100 Ω.cm. The membrane consists of a lipid bilayer having embedded proteins. Some of the proteins act as voltage gated channels for the exchange of ions. This effect is modeled by voltage dependent conductances, g_i (i=1, 2,..), in series with driving

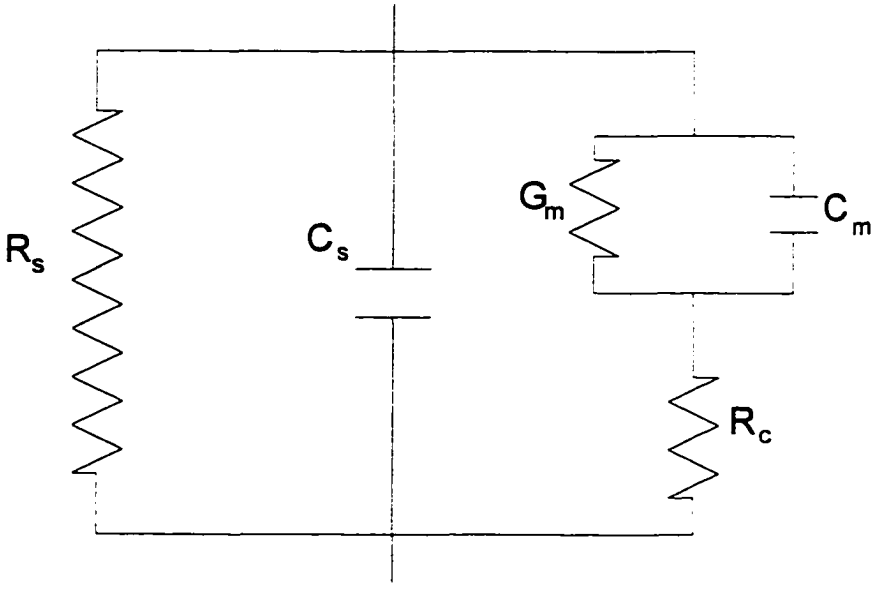

Fig. 3. Cell equivalent circuit as developed by Schwan

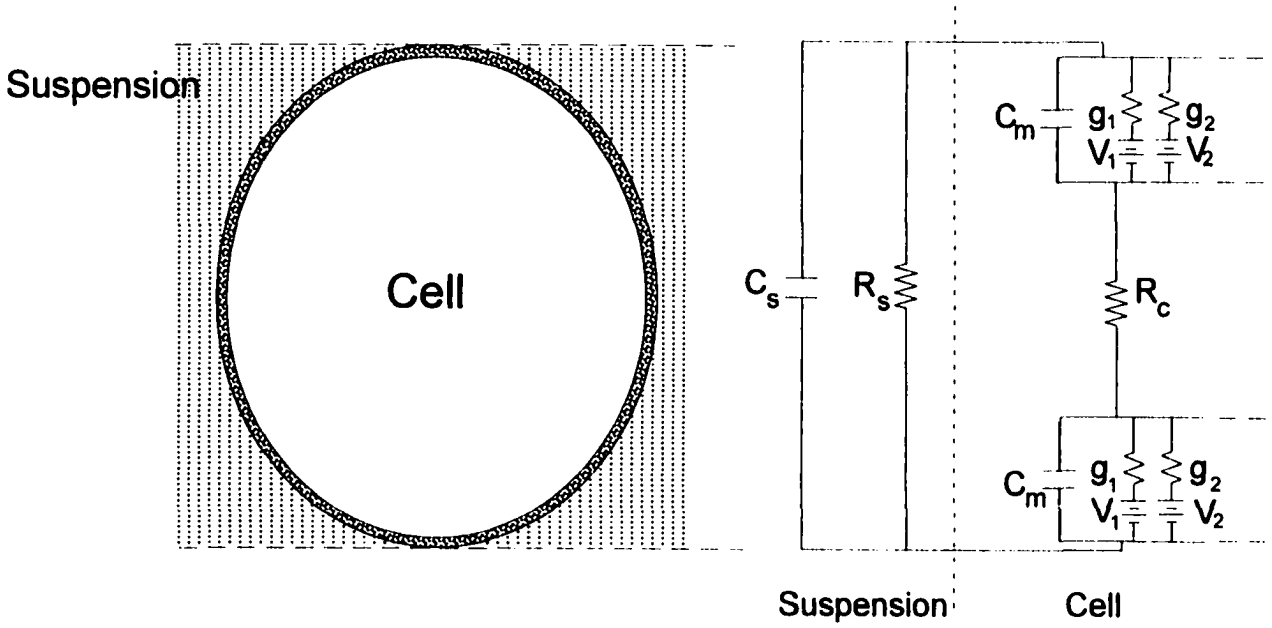

Fig. 4. Cell in suspension and modified equivalent circuit

voltage sources, V_i (Nernst potential), for each ion species. C_s, R_s are the capacitance and the resistance of the shunted suspension. The existence of the nucleus and the nucleus membrane was neglected since the effect on the outer membrane is our objective; however, it can be taken into the consideration with the same criteria.

2.3 Effect of Electric Field on Cells

Electric field can affect the selective transport of ions or molecules through the membrane; the analogy of stressing the cell is charging C_m in the equivalent circuit (figure 4). The result is a disturbance of the cell functions and, in turn, of the organism they are a part of. For low electric fields (corresponding to induced membrane voltage of around 1 V), the buildup of electrical charge at the cell membrane induces a voltage drop of about 1 V across the membrane causing voltage gating. This results in opening of channels in the cell membrane. Two types of channels exist: Sodium channels are activated first and allow influx of sodium ions into the cell. Potassium channels, which allow a flow of potassium ions out of the cell, open slowly, when the sodium channels are already in the process of closing. At this point the membrane potential begins to return to the resting membrane state. This stress is a reversible effect and its temporal range is in the millisecond range [3]. At higher fields, and correspondingly higher voltage across the cell membrane, the permeability of the membrane increases to such a level that either the cell needs from seconds to hours to recover, or cell death may occur. This irreversible breakdown of the membrane happens in nanoseconds after reaching the breakdown voltage. The most common

hypothesis is that this is due formation of pores, which allow exchange of macromolecules and such a large influx of sodium that the cell is unable to regain its ionic balance [3].

The voltage gating and electrocution effects are dependent on the amplitude and the duration of the activation pulse. Generally, the higher the amplitude of the stimulating pulse, the shorter is the response time of the channel. The relation between the electric field amplitude and the speed of the channel opening is not necessarily linear. For aquatic species, the electric field required for stunning increases sub-linearly with the inverse of pulse duration. This has tremendous consequences for large scale applications: it means that by using short, high power pulses the energy for biofouling prevention can be strongly reduced, making this process applicable for industrial applications. According to [19], the theoretical time constant for charging the membrane capacitance, C_m in the equivalent circuit of figure 3, is given as:

$$\tau_c = (\frac{\rho_s}{2} + \rho_c)\, C_m\, a \qquad (1)$$

Where a is the cell radius, ρ_s is the suspension resistivity, ρ_c is the cytoplasm resistivity, C_m is the membrane capacitance per unit area. This equation shows the dependence of the charging time on cell parameters. According to equation (1), longer pulses are needed when the resistivity of the suspension increases. Also the smaller the size of the cell, the harder to induce membrane breakdown.

Assuming that the required voltage across the membrane, V_o, necessary to achieve a certain effect, e.g. reversible breakdown, is constant, the value of

the required electric field, E_o that should be applied for a period long enough to reach steady state ($>5\tau_c$), would be [3]:

$$E_o = \frac{V_o}{1.5\,a} \tag{2}$$

The relation between an applied field of arbitrary value, E and the required pulse duration, τ, to achieve the same effect of applying E_o to the steady state is then:

$$E = \frac{E_o}{1 - \exp(-\frac{\tau}{\tau_c})} \tag{3}$$

The magnitude of the critical voltage across the membrane, which causes the onset of a certain effect on the cell - voltage gating, poration or electrocution- is dependent on the type and the size of the cell. However, typical values of critical voltage across the membrane required for reversible breakdown of most biological cells is reported to be on the order of 1 V [3]. The relation between the required voltage (or E field) across the cell to induce a voltage drop of 1 volt across the membrane, reversible breakdown effect, and the pulse duration is derived for hydrozoans. This relation is based on equations 1-3, and using cell radius of 10 μm, resistivity of salt water suspension of 50 Ω.cm, and cytoplasm resistivity of 100 Ω.cm (yielding τ_c of 125 ns), and is shown in figure 5. It shows that for this species in a salt water environment, there is an optimum pulse duration, above which no electric field reduction is obtained by increasing the pulse duration. Consequently the efficiency is expected to drop after this pulse duration. This is shown in figure 6. Among the objectives of this work is to investigate experimentally these theoretical curves.

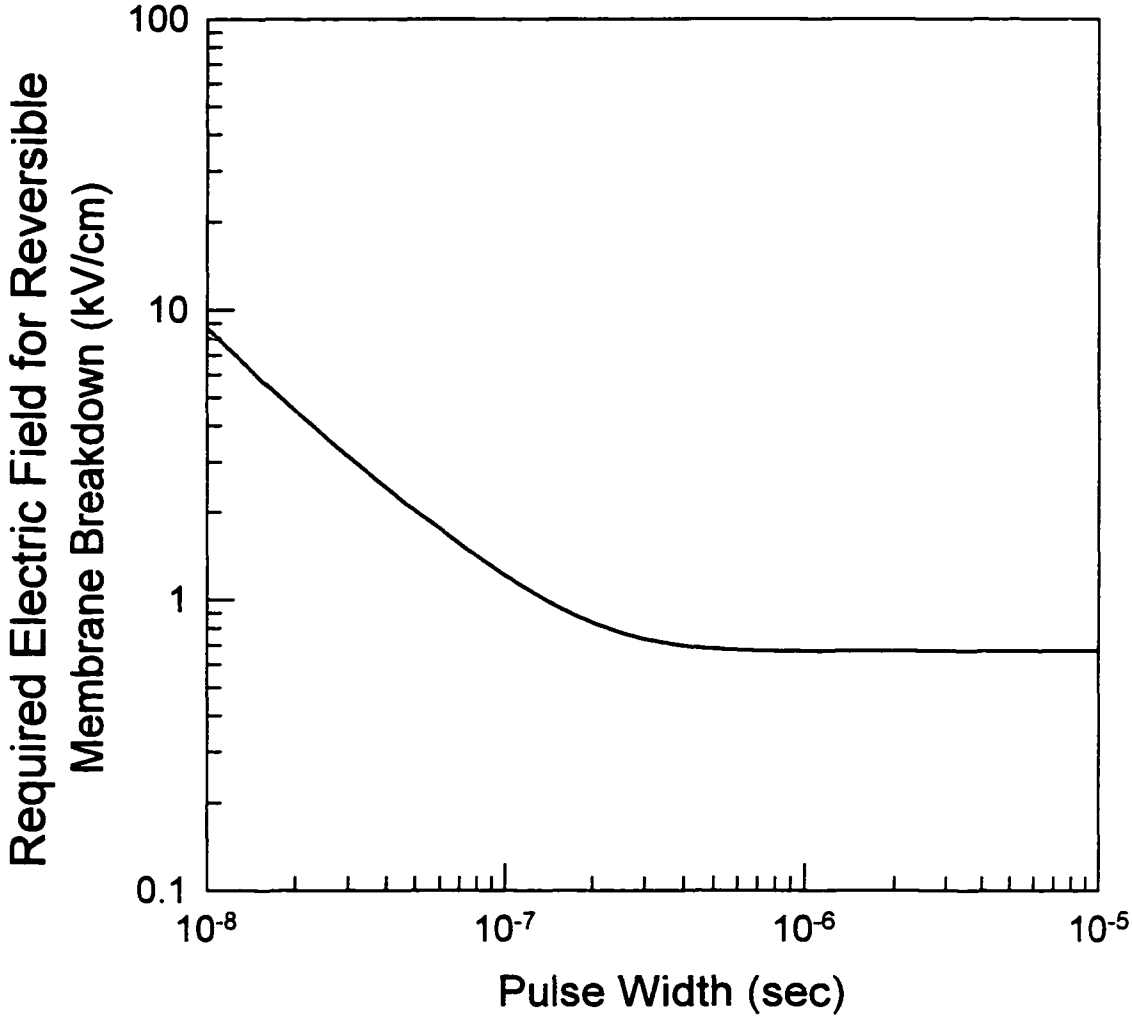

Fig. 5. Electric field requirements for reversible membrane breakdown.
(ρ_s=50 Ω.cm, ρ_c=100 Ω.cm, a=10 μm, τ_c=125 ns)

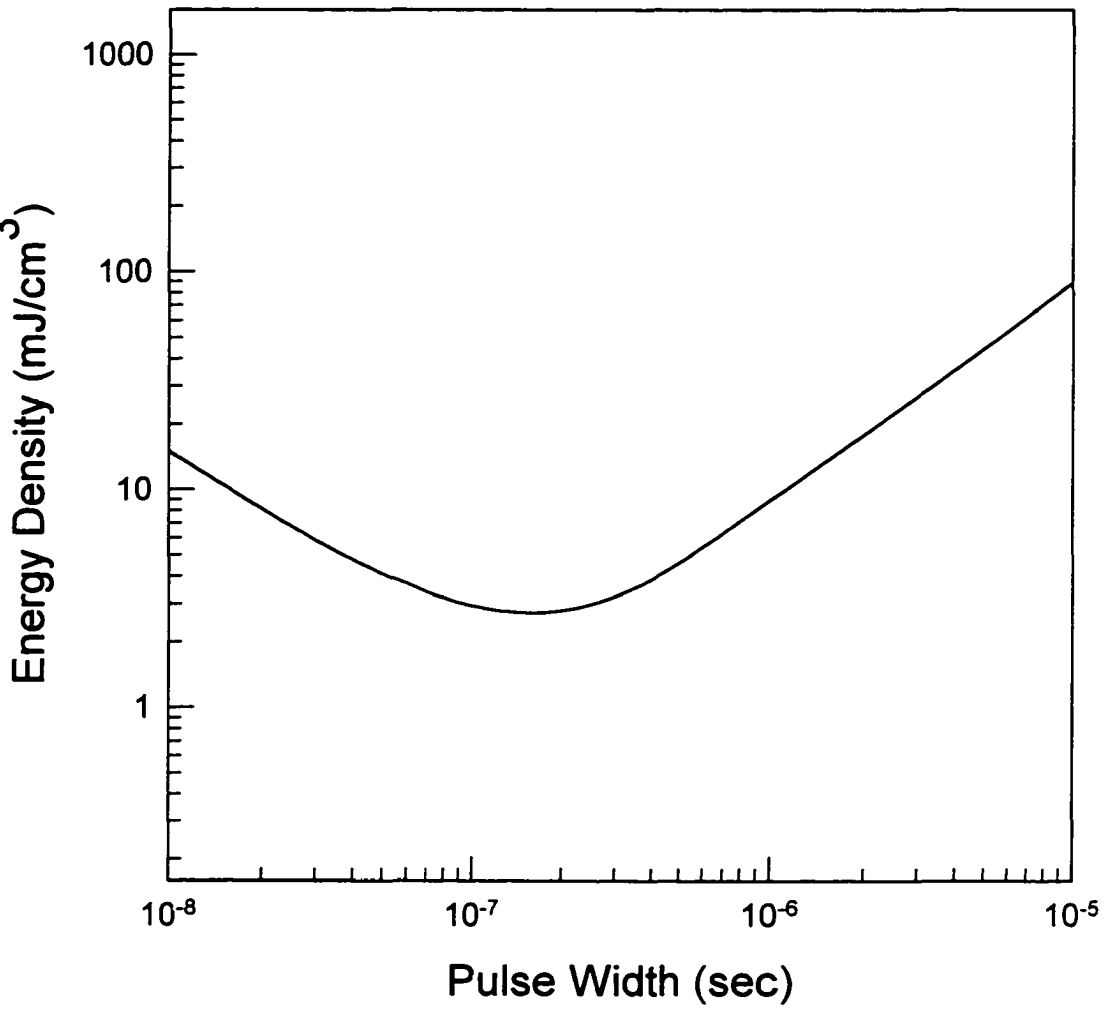

Fig. 6. Energy density required for reversible membrane breakdown versus pulse width

(ρ_S=50 Ω.cm, ρ_C=100 Ω.cm, a=10 μm, τ_C=125 ns)

CHAPTER III

EFFECT OF ELECTRIC FIELDS ON MACROSCOPIC ORGANISMS

The effect of pulsed electric fields on single cells can be extended to multi-cellular organisms. Two adjacent cells, for example, having twice the voltage difference across twice the distance yields the same value of the electric field. However, the case is not that simple in macro-organism simulations. Macro-organism anatomy ranges from multi-cellular primitive creatures, like the marine jelly fish, to complicated muscle and nerve systems in organisms like the fresh water ruffe fish. Organisms having muscle and nerve mats fall in between these two categories. In macro-organisms, other factors, compared to single cell stimulation, play an important role in the response to electrical fields. These factors include the grouping factors, interstitial fluid characteristics, and transmembrane potential distribution. It was found [18] that cell clumps of complicated geometry respond to an applied electric field with spatially-varying membrane potential changes. However, the distribution of induced membrane potential changes is considerably more complex than for single cells. Groups of cells within a clump in culture do appear qualitatively to be capable of local cooperative response to applied electric fields. The complex behavior observed in single layer clusters implies less intuitive electric field responses of tissues than single cells. However, the fact that the behavior of single cells can be understood in terms of a simple model, provides guidelines for the tissue stimulation mechanism, and the stimulating parameters.

Many investigations in effects of electric fields involve multi-cellular structures. Examples include macroscopic organisms, the heart, which has on the order of 10^{10} cells, and whole muscles. In modeling the electric behavior of such preparations, the discrete cellular structures may be important, but is very complex to analyze. For accurate modeling, one can introduce the potential and current field variations on a cellular scale, which are superimposed on variations that take place over longer spatial distances. Usually, this is of little interest when studying the macroscopic behavior of certain structure, and an averaged continuum associated with the averaged fields is an acceptable and even a desirable simplification. Consequently, macroscopic fields (averaged) may be adequate to describe the phenomena of interest. In this case, it is possible to replace the discrete structure with an averaged continuum that represents a considerable simplification (Volume conductor theory). The parameters of the continua are derived by a suitable average of the actual structure. The membrane separates different domains at each point. The region of application of this simplification differs from one system to another. In macroscopic organisms, the whole organism may be considered as a conducting region that surrounded by the capacitive membrane. In larger systems, they can be considered as islands of different characteristics separated by bones for example. Cardiac tissues were replaced by intracellular and interstitial continua domains occupying the same physical tissue space (Bidomain model [1]). Averaged electrical characteristics were derived for different kinds of tissue [2]. Maxwell equations, based on the electrical properties of these biological

structures and the characteristics of the source of the field with the appropriate boundary conditions, can yield the current and the potential distribution throughout this volume conductor. A rough estimate of the current density threshold that can disturb biological systems was found to be on the order of 10 mA/cm^2 when applied for few seconds [2].

Studying the effects of electric fields on a whole macroscopic organism is much more complex problem than studying single cells. This is due to the complexity of the biological systems and their feedback mechanisms that tend to null out any perturbations resulted from field application. For example, cooling mechanisms of the organism reduce the increase of temperature resulting from certain energy deposition to a small fraction from the calculated value. However, existence of electric field effects on biological systems is doubtless. Decreased rate of growth and fatigue of rats exposed to 1 kV/cm electric field for 30 days has been reported [10]. An increase of 64% mortality in honeybees was reported with an exposure to 4.5 kV/cm electric field [2]. Significant change in dogs' blood chemistry was reported as a result of exposure to 0.25 kV/cm for 8 hours per day for six weeks [2]. Analysis of field effects on these living systems is very complicated problem and requires a lot of simplification. However, some guidance can be obtained by working up from the cell level to more complex structures.

Chapter IV

BIOFOULING ORGANISMS

4.1 Introduction

The macroscopic fouling organisms include all those in which the individuals, or the colonial masses formed by them, are large enough to be recognized by the unaided eye. There are `numerous kinds of these organisms between hard shell organisms and organisms without shells. However, I will introduce a basic background about a few of them that were the essential targets in my study.

4.2 Hydrozoan

A salt-water hydrozoan (*Stylactis arge*) was chosen to be the species for our laboratory experiments for many reasons, which include:

1) It is a major biofouling organism in marine systems and there is a wide interest in getting rid of its problems.
2) It offers the possibility to evaluate stress strength due to a certain stimulus, through measures of body and tentacles contraction and expansion.
3) It has a short doubling time, only a few days.
4) Its food in the laboratory, *Artimea salina*, is readily available.
5) Animals grown asexually by budding are genetically alike, so similar stimulation can be expected.

For the purpose of electrical stimulus analysis, a very primitive look at the hydrozoan anatomy will be introduced. A more specialized biological analysis of these species can be found elsewhere [7]. Hydrozoans exist as polyps, i.e., as

sedentary forms of coelenterates. A single animal has the form of a tube, sub-mm long and 0.05-0.2 mm wide, bearing a whorl of hollow tentacles near one end with the mouth in the center of these tentacles. Figure 7 shows a picture of a typical hydrozoan. The whole body is enveloped in a tri-layer soft wall consisting of two layers of different cells with a plasma membrane between them. The basal disk, at the rear part of the body, secrets a sticky material that fastens the animal to a substrate. This species consists of about 20 different cell kinds; there are a total of fifty thousand cells per animal. Excitable cells, muscle cells and nerve cells, are the targets of our electrical stimulus. The muscle cells are found in a sheet of parallel, adjacent cells called muscle mat. These cells exist in the whole body regions and are transformed in many ways to perform different functional tasks. Their sizes are in the range of few micrometers. Nerve cells are small cells, about 10 μm, with about two to five slender emanating from the cell body [8]. The nucleus of a nerve cell is condensed, and the cell body has little cytoplasm. Most of the nerve cells form a nerve net in the interstitial spaces just above the muscle mat.

4.3 Barnacles

Barnacles are one of the most familiar biofouling organisms found attached to ship bottoms. They are nearly distributed worldwide in tropical and warm temperature seas. They attach to surfaces in the larval stage and then the body changes its characteristics to adult form. In their adult form, they are encased in hard shells and are permanently attached to surfaces which are completely submerged or periodically wetted. The opening of the shell can be

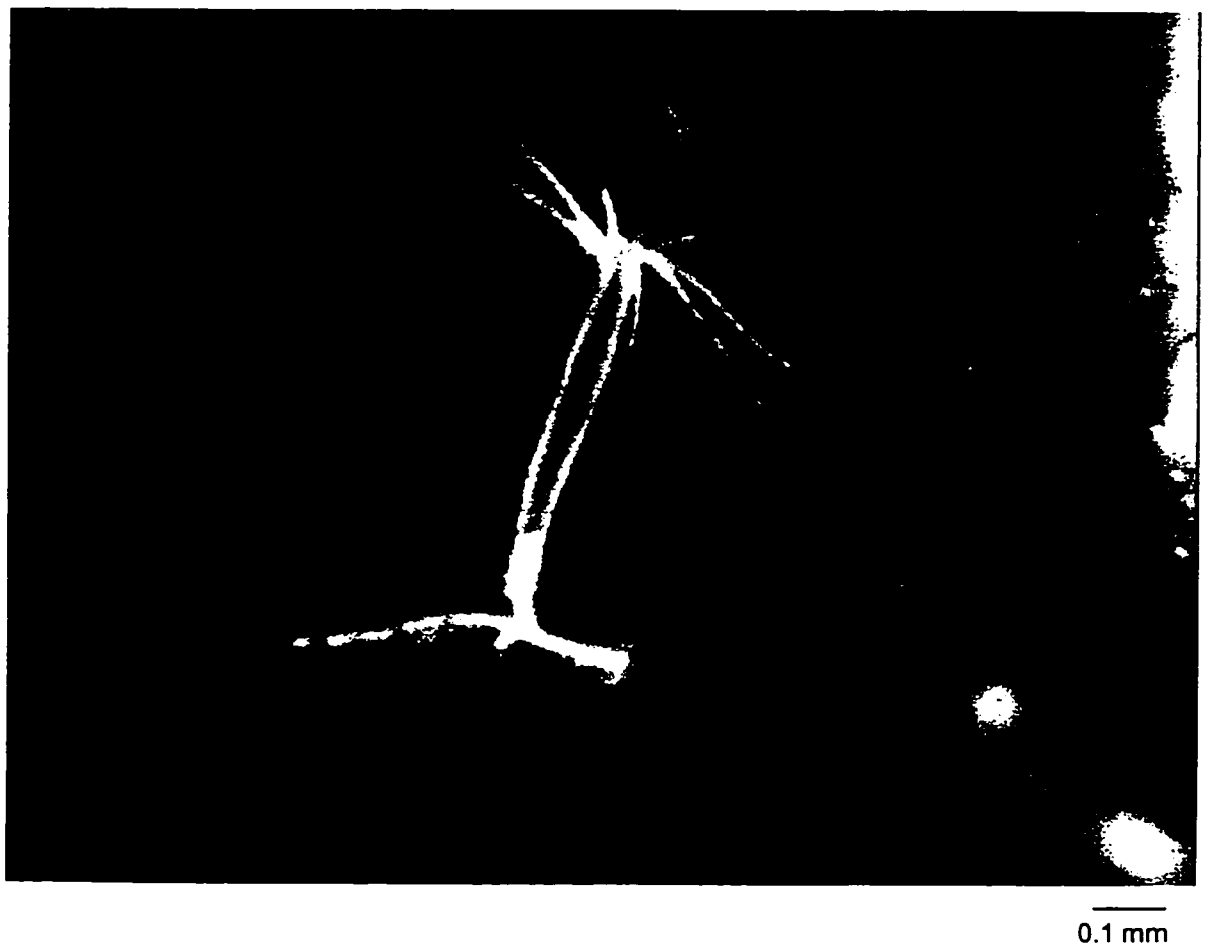

Fig. 7. Picture of salt water hydrozoan (*Stylactis Arge*)

closed by two moveable covers. They feed by extending their legs through this opening of the shell and sweeping the adjacent water for food. Most barnacles reproduce by cross fertilization. Masses of sperm are deposited in the mantle cavity of one individual by its neighbor. The eggs are shed into the same cavity, where fertilization takes place. Development proceeds within the mantle cavity for varying lengths of time depending on species, temperature, and locality. Figure 8 shows a picture of a typical salt water barnacle.

4.4 Zebra Mussels

Zebra mussels are small, fingernail-sized mussels native to the Caspian Sea region of Asia. They were discovered in Lake St. Clair near Detroit in 1988. Zebra mussels have now spread to all the Great Lakes and are showing up in many inland lakes in North America. Female zebra mussels can produce between 40,000 to over 1 million eggs per summer. These develop into microscopic, free-floating shelled larvae called veligers and post-veligers. At about three weeks the sand grain-sized larvae start to settle and attach to any firm surface using "byssal threads". They will cover rock, metal, rubber, wood, docks, boathulls, native mussels, and even aquatic plants. As a result they have clogged water systems of power plants and water treatment facilities, as well as irrigation systems. The zebra mussel grows up to two inches in length, with an expected life span of five years. The adult mussel feeds on plankton by filtering water at a rate of one liter per day. The long-term economic impact of zebra mussel has been calculated in billions of dollars [11]. Figure 9 shows different life stages of the zebra mussel.

From sea grant web site with permission

Fig. 8. Picture of salt water barnacles (Goose Neck)

Zebra Mussel Veligers in Free Floating Stage Under Microscope

Adult Stage with Byssal Threads

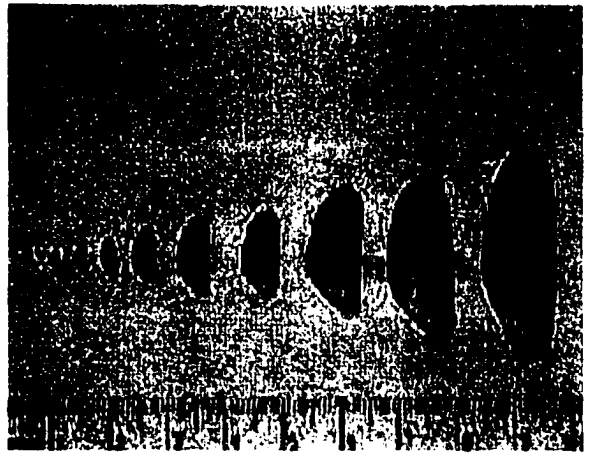

Zebra Mussel Adults Ranging from Pinhead Size to 3 cm

Fig. 9. Zebra mussel in different life stages
(from sea grant web site)

CHAPTER V
LABORATORY EXPERIMENTAL WORK

5.1 Objectives

One objective of this work was to optimize stimulating parameters to achieve the required stunning duration for biofouling organisms. These parameters include pulse width versus pulse amplitude, pulse frequency components, and pulse repetition rate. The relation between the pulse width and the magnitude to achieve certain effects, stunning or electrocution, was be investigated via laboratory experiments and compared to the theoretical criteria shown in figure 5. Effect of pulse frequency components on stunning duration was illustrated via comparison between the stunning effects of rectangular pulses and sine wave pulses. Figure 10 shows the frequency components of equal energy rectangular pulses and sine wave pulses. It shows that high frequency components of rectangular pulses have higher amplitude than the corresponding components of sine wave pulses. The higher frequency components in the rectangular pulses, up to a frequency corresponding to the time constant of the membrane charging ($1/\tau$), are expected to have longer stunning duration, due to decreased impedance of the plasma membrane capacitance to these components.

Pulse repetition rate is another important parameter required to achieve maximum effects of pulsed electric field. Resealing of pores caused by the electric field pulses are reported to occur in the millisecond range [3]. Consequently, applying the consecutive pulses before this resealing process

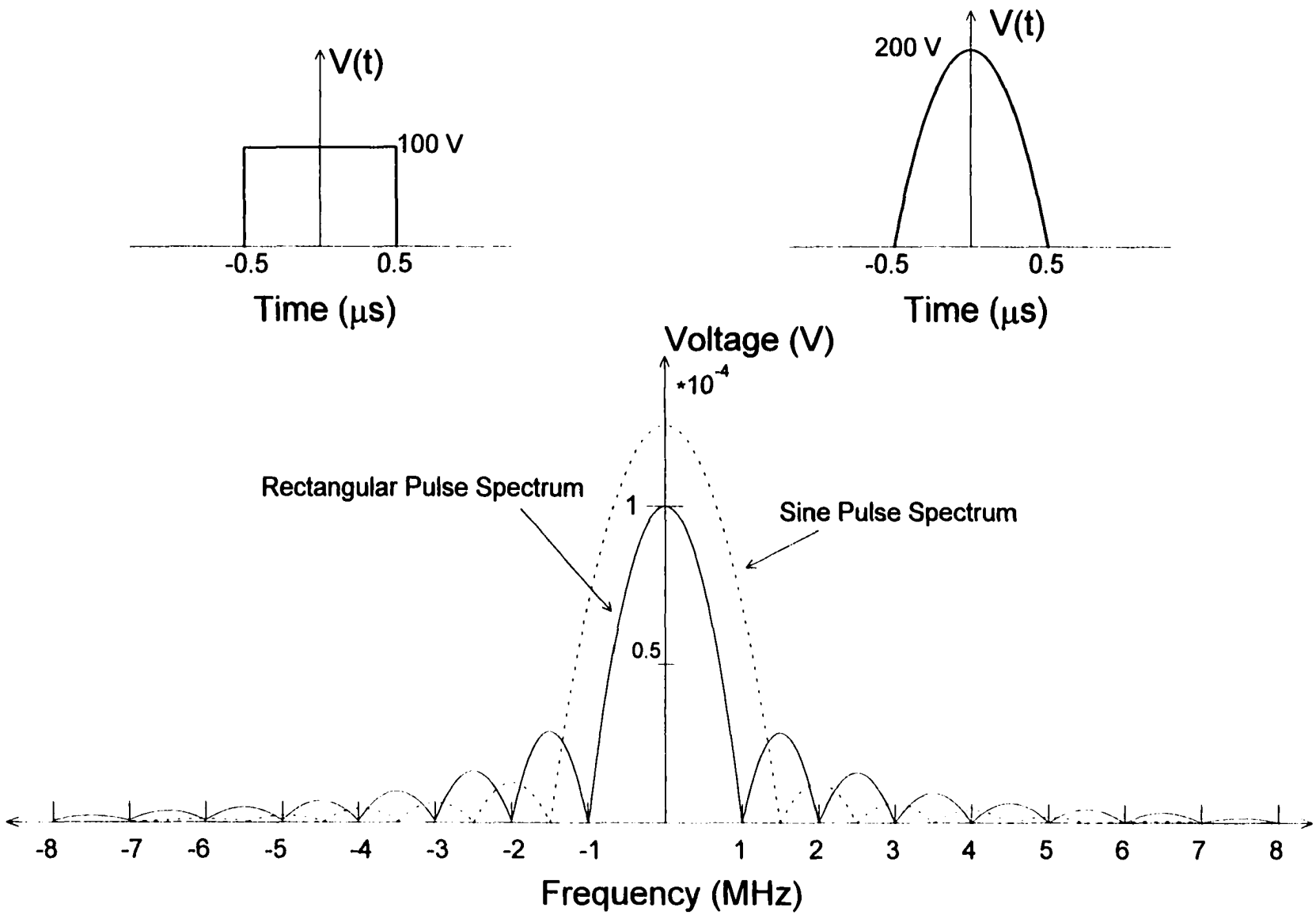

Fig. 10. Spectrum of equal energy rectangular pulse and sine wave pulse

is complete will yield cumulative effects and higher efficiency. On the other hand, applying the consecutive pulses after the resealing of pores is complete is merely a repetitive effect of one pulse or even worse, as these pulses may be applied in the refractory period, immediately after the stimulation in which the cells are not excitable. The response of the hydrozoans to variations in these parameters were verified by laboratory experiments as well. Long term effects, in terms of ability of feeding and late mortality, were investigated in our laboratory experiments. Finally, design recommendations for large scale systems, based on lab work, were utilized in our field experiments.

One advantage of using short pulses is that thermal effects can be disregarded. Thermal effects are usually taken into consideration in the millisecond range pulses [13]. Polarization effect of the suspension can also be disregarded when applying microsecond pulses. The capacitance C_s and the resistance R_s describe the capacitive and resistive properties of the suspension. Generally, for low concentrations of organisms in the suspension, the time scale of the polarization of the suspension (dielectric relaxation time) determines the lower limit in pulse duration for membrane effects. The time constant for polarization is given as the product of the dielectric constant and the resistivity. Water, which is the suspension of aquatic nuisance species, has a relative dielectric constant of 81. This gives dielectric relaxation times for salt water (ρ = 50 Ω.cm), and fresh water (ρ = 3 kΩ.cm) of 0.35 ns and 21 ns respectively. Consequently, this consideration can be disregarded with the use of longer pulses needed to charge the membrane capacitance.

5.2 Experimental Setups

To meet the objectives of laboratory experiments, a wide range of field parameters need to be investigated. The effect of pulses with duration from hundreds of nanoseconds to few microseconds needed to be studied. The range of field strength reaches up to tens of kilovolts per centimeter. Effects of sine wave pulses and rectangular pulses were compared. Due to this wide parameters range, four different pulse generators were used in this study. They are described in the following:

5.2.1 Line type pulser with laser triggered spark gap switch

In order to generate 300 nsec electrical pulses with field strength up to 20 kV/cm, a line type pulser with laser triggered spark gap switch was used. The pulse forming network was parallel connected coaxial cables. Five 50 Ω cables of 30 m length each were charged to a voltage V_o by means of a DC power supply. The energy stored in the cables was transferred into the load by closing a laser triggered spark gap with a rise time of approximately 10 nsec. The pulse amplitude is $V_0/2$ for a matched load, where the resistance of the suspension is identical to the impedance of five parallel cables (Z=10 Ω). The applied voltage could be varied up to 20 kV, providing maximum pulse amplitude of 10 kV across the load; pulse width was fixed at 300 nsec. The electric field in the cuvette is given as Vo/2d, where d is the distance between the two aluminum electrodes. With distance of 0.2 cm, the maximum electric field is 50 kV/cm. However, surface flashover at the suspension surface limited the maximum field to about 20 kV/cm. A schematic diagram for this pulse generator is shown in figure 11. Physical layout and a real time pulse are shown in figures 12 and 13 respectively.

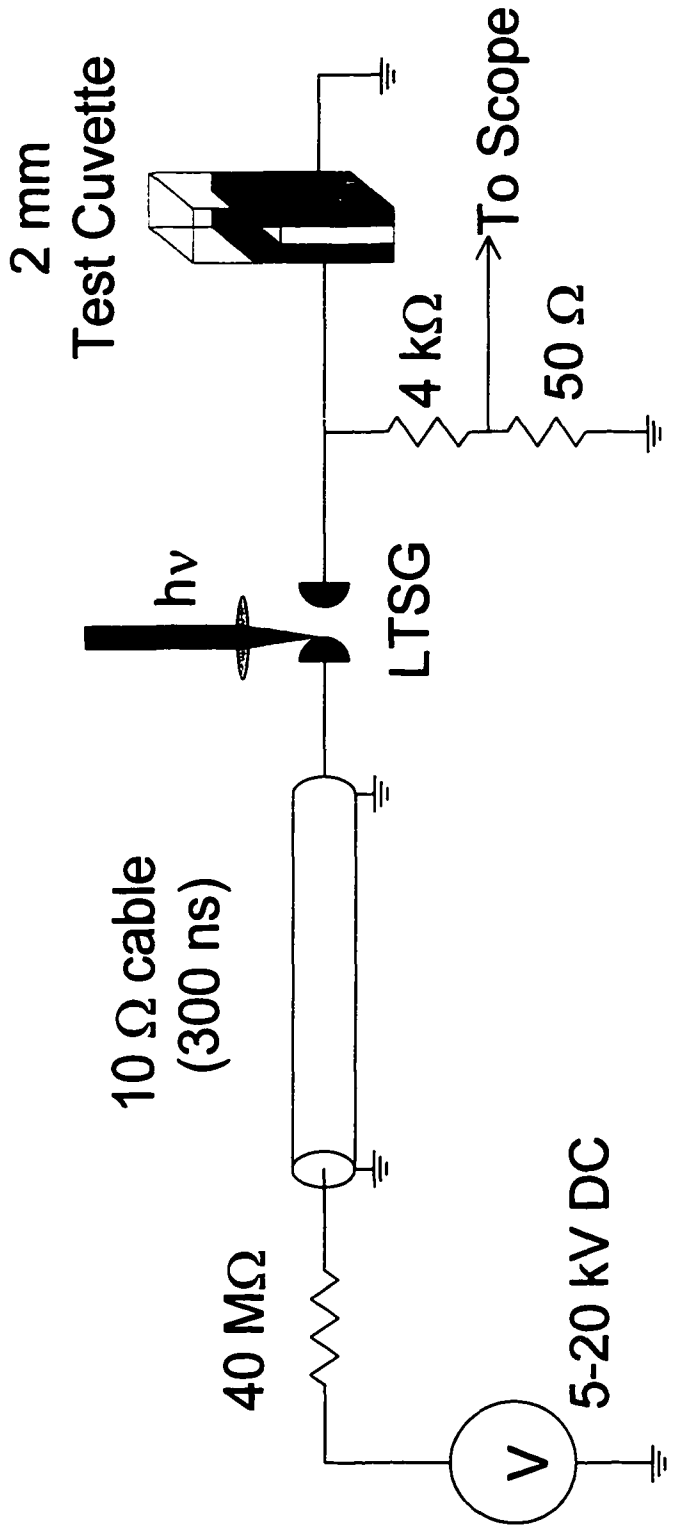

Fig. 11. Schematic diagram for the laser triggered spark gap pulser

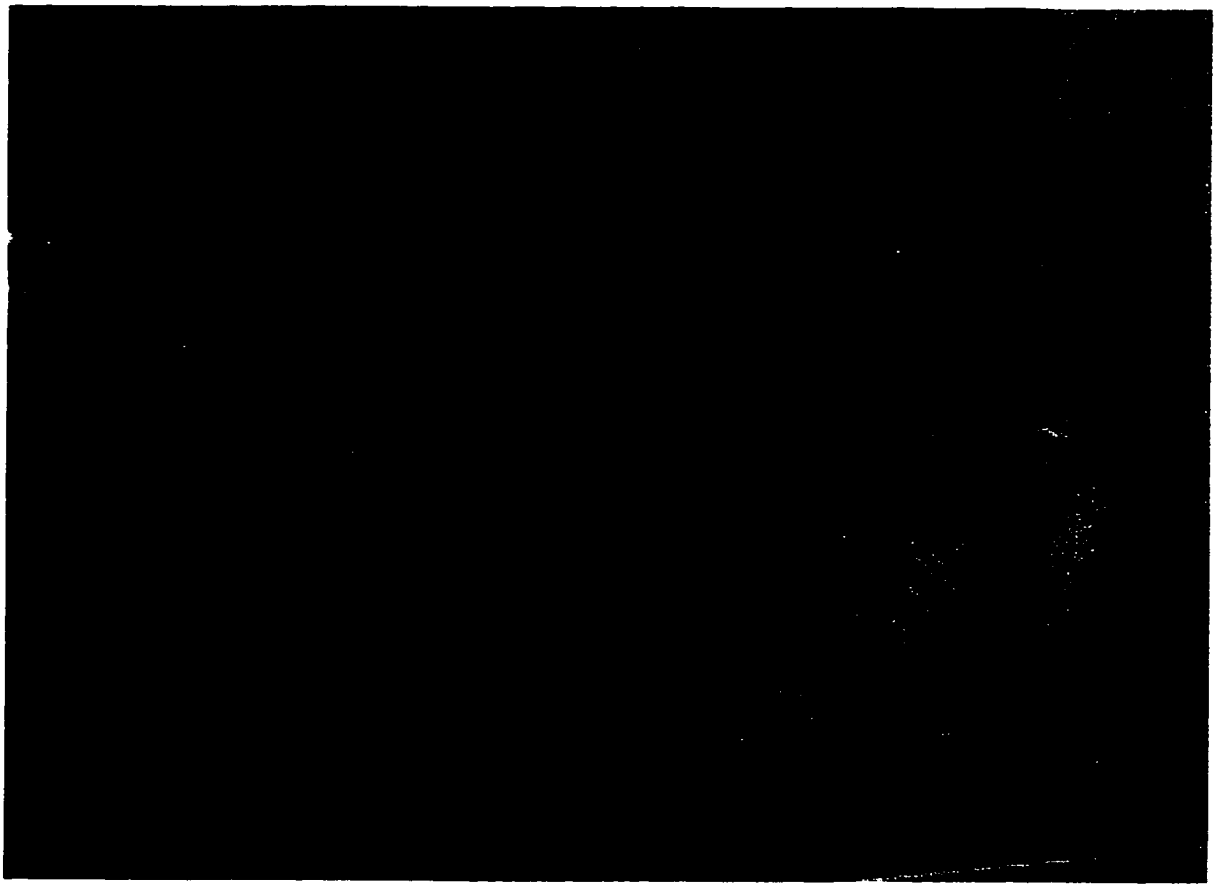

Fig. 12. Physical layout of the laser triggered spark gap pulser

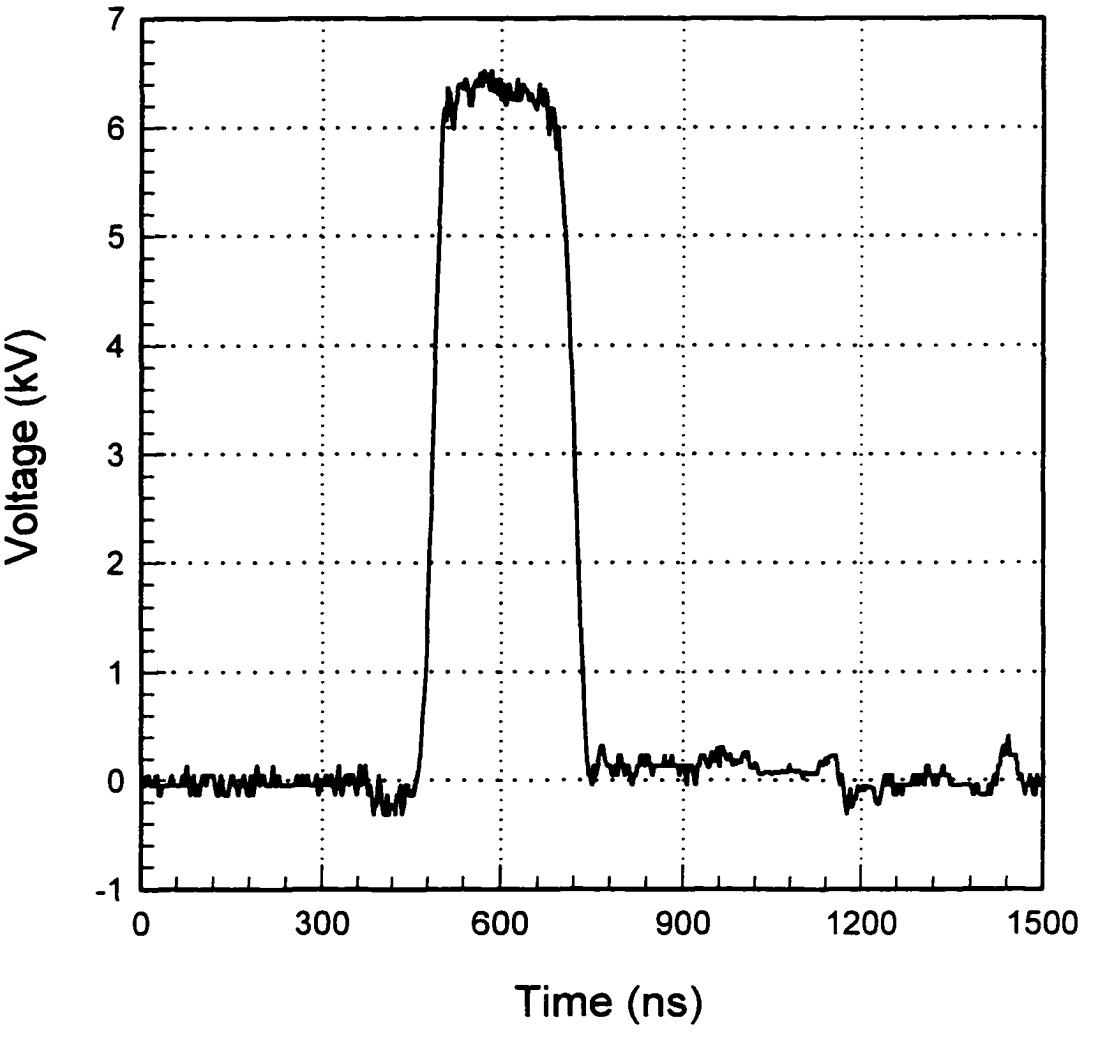

Fig. 13. Real time pulse from the laser triggered spark gap pulser

5.2.2 Line type pulser with thyratron switch

For longer pulse width and higher energy deposition, a line type pulser was constructed utilizing a gas tube switch, the thyratron (has a typical life time of 10^9 shots). The pulse forming network in this pulser consisted of 25 parallel capacitors, 2 nF each, connected with series inductances of 0.2 μH each, giving a pulse width of 1 μs and a characteristic impedance of 10 Ω. The pulse forming network capacitors was charged via a constant current power supply (Maxwell type CCDS CS080). Energy stored in the PFN was released into the load via a thyratron switch (type EG&G HY3003) with a rise time of about 50 nsec. Thyratron heating and trigger requirements were provided from high current transformer and EG&G thyratron controller respectively. Underdamping protection circuit was introduced to protect the power supply from current swinging. Electric fields up to 62.5 kV/cm were theoretically obtainable with charging the pulse forming network to 50 kV and using cuvettes of 0.4 cm gap distance. However, the maximum needed value of the electric field was 20 kV/cm. No flashover was experienced up to this value. For low electric fields experiments, under 5 kV/cm, thyratron continuous conduction was noticed due to the overlap between the recovery process of the thyratron and the beginning of the next charging cycle by the power supply. To overcome this short circuit, inductance of 100 μH was introduced in the charging circuit and the resistance was adjusted to give just overdamped charging. This enabled us to trigger the thyratron at low voltages. Figure 14 shows a schematic diagram for this pulser. Physical layout and a real time pulse are shown in figures 15 and 16 respectively.

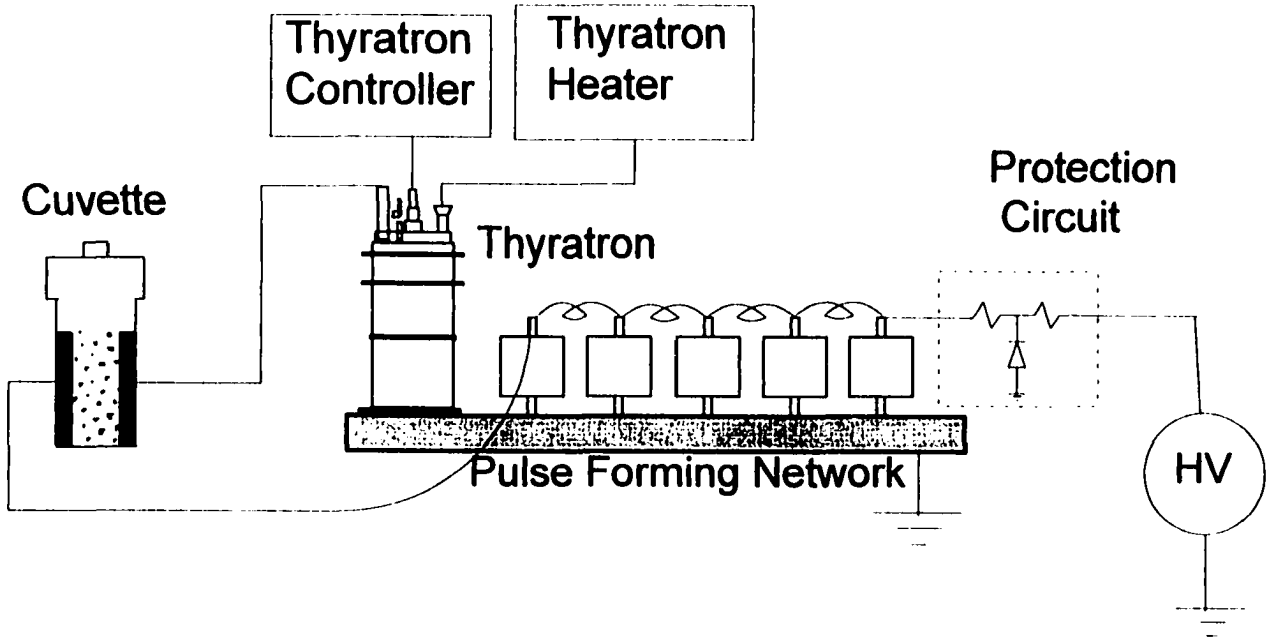

Fig. 14. Schematic diagram for the thyratron pulser

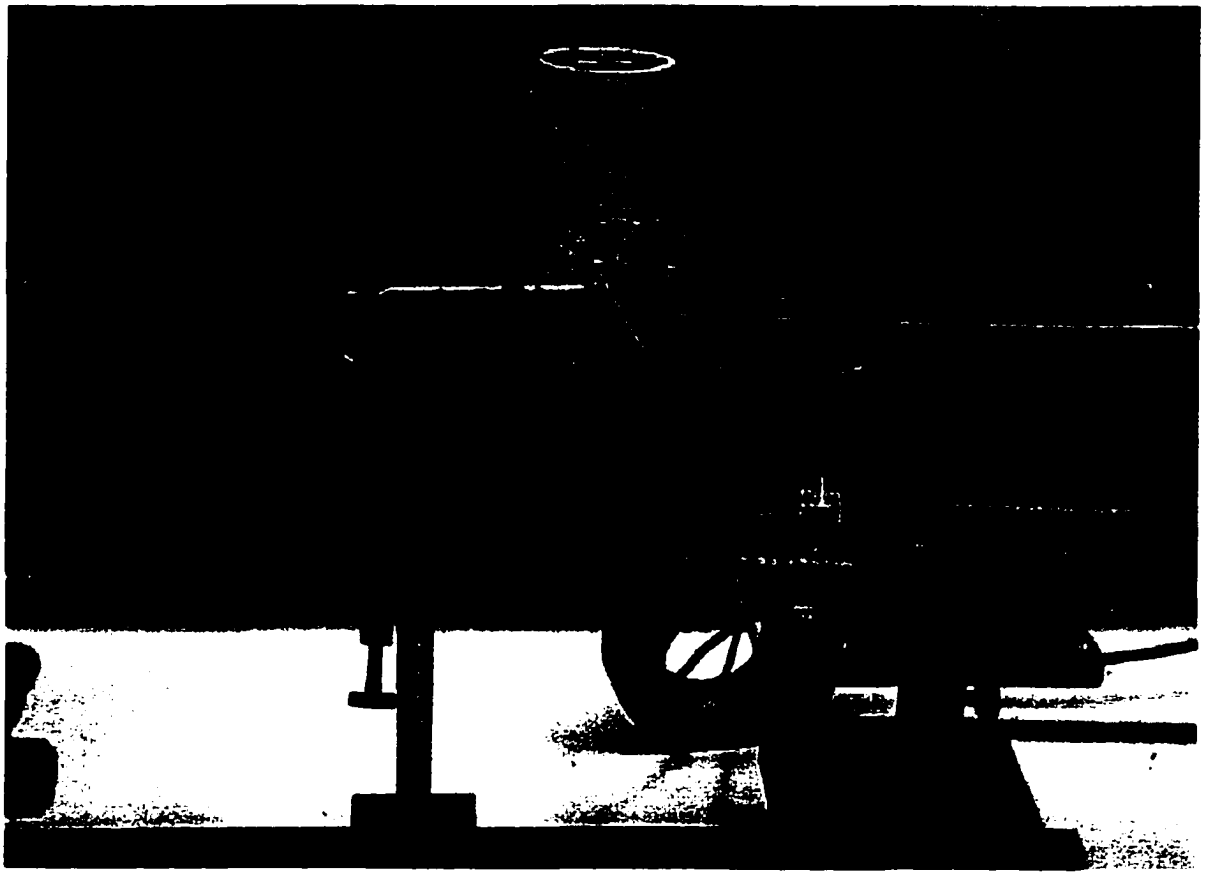

Fig. 15. Physical layout of the thyratron pulser

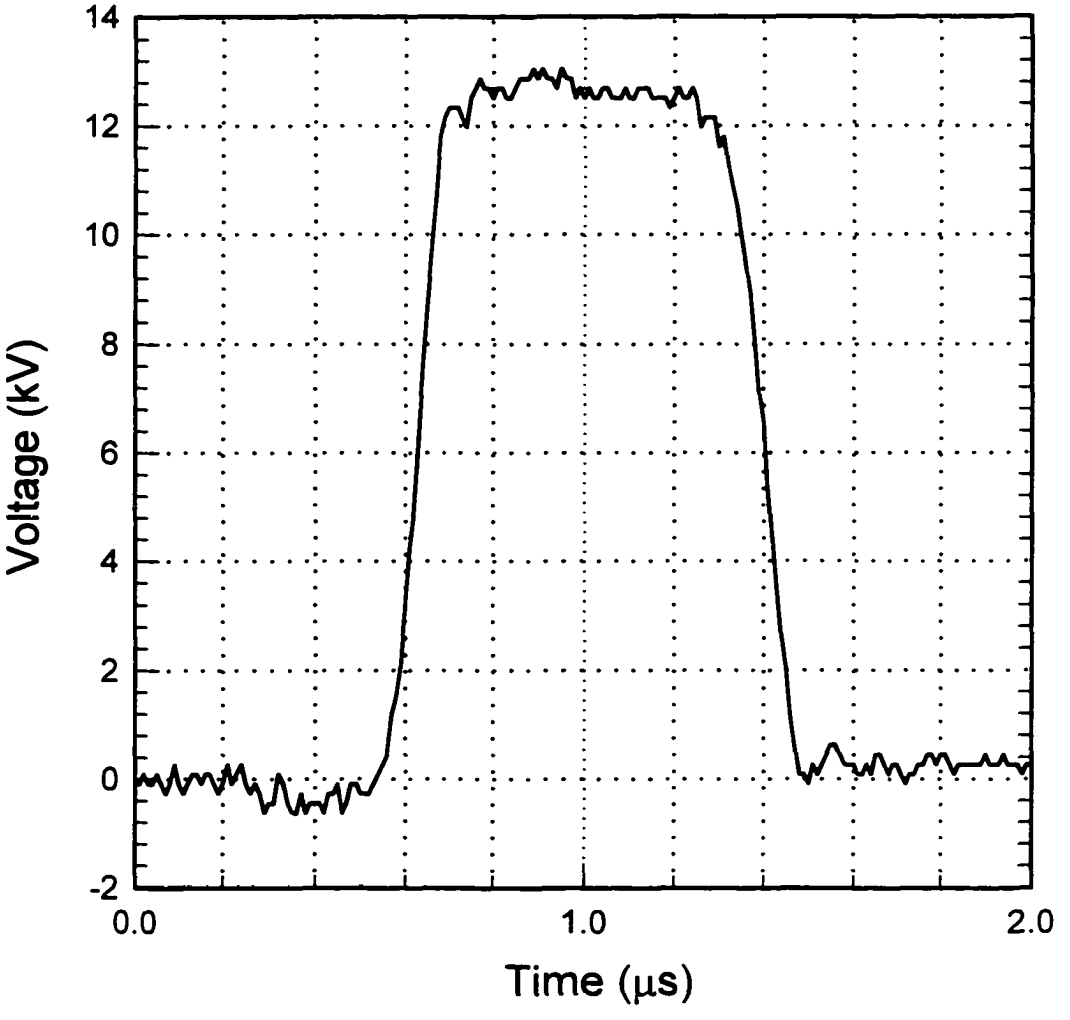

Fig. 16. Real time pulse from the thyratron pulser

5.2.3 Hard tube pulser with MOSFET switch

For low electric fields, below 3 kV/cm, a hard tube pulser was built using a high speed density capacitor and a semiconductor MOSFET switch. The parameters of pulse duration and pulse amplitude were adjustable which allowed for greater flexibility in the range of tests performed. A "hard tube" type pulser was selected over a pulse forming network, which has a fixed pulse width. The circuit was designed so charge through the load was avoided. The pulsed power switch has the characteristics of turning "on" and "off" very fast, on the order of 50 nsec. The switch follows a trigger pulse and stays in the conducting state for the duration of that pulse. By varying the length of the trigger pulse, the pulse duration of the pulser circuit was varied. The amplitude is varied simply by adjusting the voltage level on the power supply connected to the energy storage element. The pulser was made safe by adding a "bleeding" resistor bank in the circuit to discharge the capacitor when it was not being discharged and also by enclosing the entire design in a sealed Plexiglas box.

The performance of the circuit is dependent on the capabilities of the semiconductor switch. The discharge of an energy storage element has the shape of an exponential decay and is given by the formula $\tau = RC$. In order to obtain a square pulse, the switch must be able to turn on and off in a small fraction of the total discharge time. A power MOSFET (type Harris IRFPG40) was selected for the short pulses for its superior switching speed characteristics, an IGBT (type Harris 15N120C3) was selected for longer higher voltage pulses and for its superior low conduction losses. The maximum current is determined by

both the switch and the load resistance. The switches allowed me to generate a square pulse of up to 1200 volts and τ = 10 μs into a load resistance as low as 10 Ω, corresponding to salinity of 20 ppt (suitable salinity for the salt water species). The capacitance was 13.5 μF. The generation of short pulses (nanosecond) is limited by the inductance of the circuit. The inductance was minimized by making the physical connections to the main discharge loop as short as possible and by choosing an energy storage element with a geometry which has minimum inductance. A schematic diagram of the pulser circuit is shown in figure 17. Physical layout and real time pulse are shown in figures 18 and 19 respectively.

5.2.4 Sine wave pulse generator

Sine wave pulses were generated using a high voltage pulse power generator supplied by Megapulse, Inc. This generator uses the patented high power modulator (megatron) technology that was developed and implemented in the transmitters that form the national Loran-C radio navigation and position fixing system. Advantages of this pulser include extreme reliability, robustness, efficiency, and ability to work for wide range of load impedance. The generator was able to generate sine wave pulses with 5 μs width and different polarities, with voltages up to 20 kV. Frequency control was also possible through simple push buttons. Over-current protection was equipped, max current was limited to 100 A.

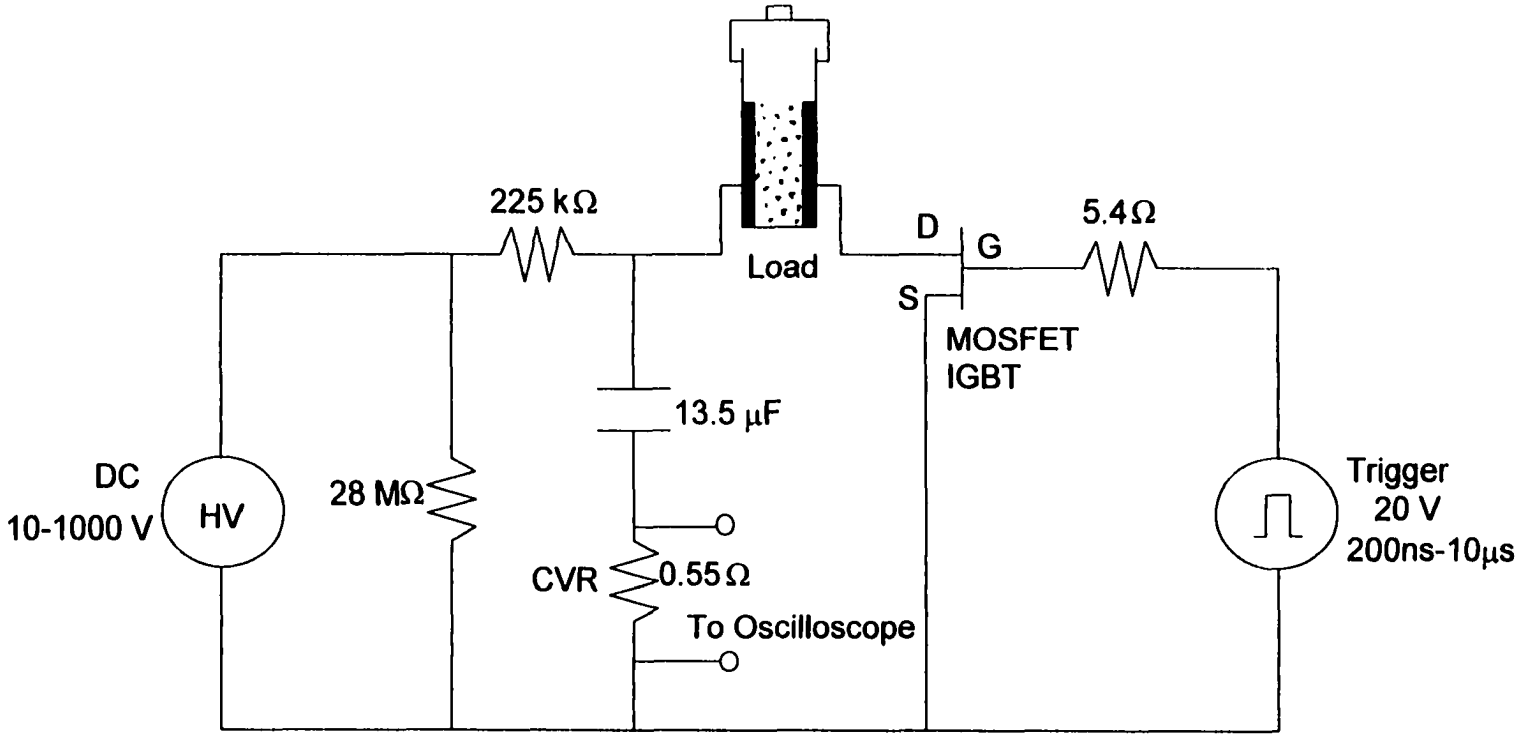

Fig. 17. Schematic diagram for the hard tube pulser with semiconductor switch

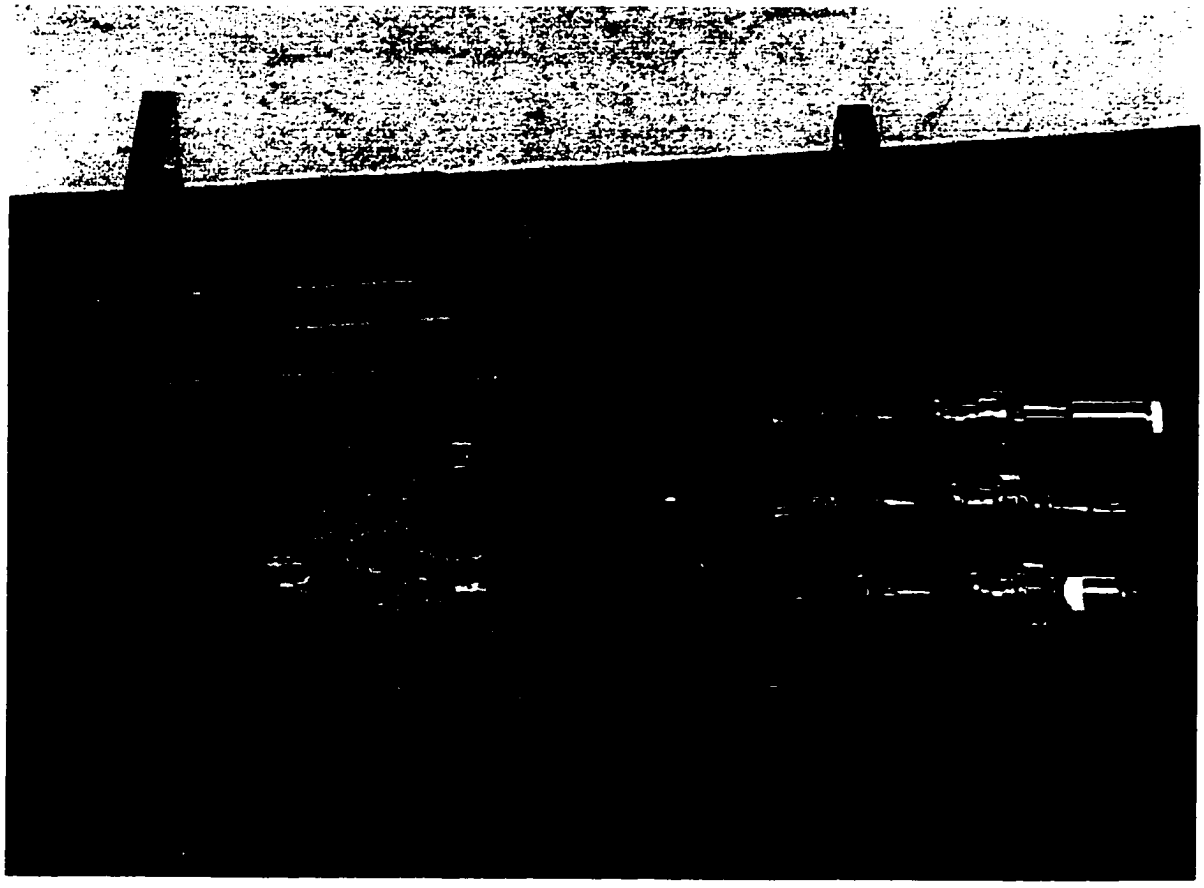

Fig. 18. Physical layout of the MOSFET pulser

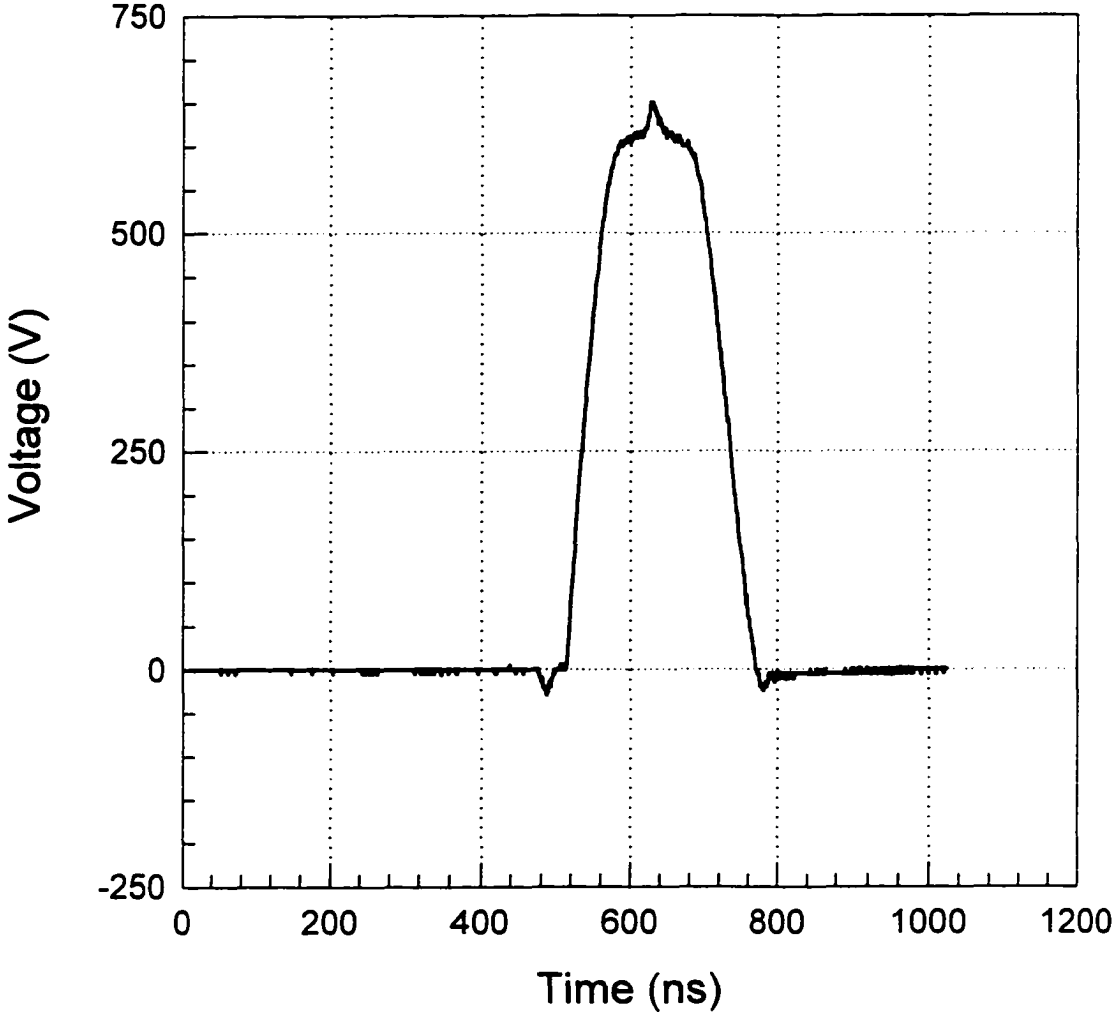

Fig. 19. Real time pulse from the MOSFET pulser

5.3 Diagnostics

In all setups, the optical diagnostics were performed by using a CCDS camera monitoring system. Magnification up to 120x was available, which is enough for the sub-millimeter organisms. Cuvettes having aluminum electrodes of dimension 1x2 cm and 0.4 cm electrode separation were used in most experiments, however, a few experiments utilized 0.2 cm separation distance to obtain higher energy density with less current. The output of the camera was recorded by Monitor-VCR system, and a computer interface snappy program.

The electronic diagnostics of the current were done by a pulse current transformer from Pearsons Electronics Incorporation (model 110) with an output of 0.1 V/A. Monitoring of this current was done using Tektronics oscilloscope (model 2232) which was serially connected to the computer for recording purposes.

5.4 Experimental Procedure

Hydrozoans were collected from the Applied Marine Research Laboratory, where they grow in fish tanks and feed on its residuals. The hydrozoans were defined as *Stylactis arge*. Similarity to the field biofouling hydrozoans was also verified. A suitable environment was prepared in the Physical Electronics Research Laboratory, with salinity of 20 ppt, and a bubbling air sources. Freshly hatched brine shrimp was fed to the hydrozoans about three times a week, corresponding to experimental needs. The hydrozoan polyps were separated mechanically, then transferred to cuvettes using a pipet. After transfer, they were left for one day before any experimental procedure to relieve any stress due to

the dissociation and transfer process. At the time of the experiment, the organism usually was unfed for one day to ensure expansion of its tenticals. Response to electric pulses was easily recognized; rapid movement of tentacles into the body and body contraction to almost one third the original length are direct responses to the electrical pulses. Evaluation of the stunning period was based on these motions; a stunned hydrozoan was considered to have recovered when the contracted body and the retracted tentacles reached about 80% of the length before stunning. This evaluation become more accurate when the observer became trained. Because this study was stochastic in nature, five experiments were run for each set of parameters, and the average stunning time was reported. Monitoring the hydrozoan for five minutes before the application of the pulse was done to ensure normal activity, the recovery process after the pulse was also monitored.

5.5 Results

5.5.1 Effect of Electric Field Strength and Pulse Width

The first step in determining the effect of electric field strength on hydrozoan stunning period was to determine the lower and upper limits of stimulating fields, i.e., the minimum stimulating electric field and the field required at some pulse duration, to cause mortality. The laser triggered spark gap pulse generator with 300 nsec pulse width was used first for this objective. The minimum field strength to stimulate the hydrozoan was 0.5 kV/cm for which it had a stunning period of 0.5 minute. However, the maximum obtainable field strength with this pulser was 20 kV/cm, which was not enough to cause mortality at this pulse width. Consequently, the 1 μs thyratron pulser was used to determine a

lethal dose of electric field, and it was found to be 20 kV/cm at 1 μs. Mortality consistently was associated with the release of material from the mouth region of the hydra. This material may have been food or a parasite.

The next objective was to define the pulse width range that gave maximum efficiency, i.e. having the same stunning duration with less energy expenditure. This was done by pulsing the hydra with different pulse widths, and changing the field strength gradually to reach a constant stunning time (conservatively set in this experiment at 5 minutes). These experimental data are tabulated in table 1 and graphed in figure 20.

Table I
Energy expenditure for different pulse width to achieve 5 minutes stunning time

Pulse Width τ (μs)	Electric Field to Achieve 5 min. Stunning Time (kV/cm)	Energy Density (mJ/cm^3)
0.050	12.5	230
0.300	3.5	100
1	3	257
9	1.4	495
25	1	714

It can be concluded from figure 20 that the pulse width for maximum efficiency lies in the range of few hundreds of nanoseconds. This result is consistent with reference [19], and with the theoretical curve shown in figure 5. Consequently, most of our experiments have been performed with pulse duration of approximately I μs.

A series of experiments were done using different pulsers and pulse widths to investigate the effect of field strength on stunning duration in the range of 0.5-20 kV/cm. These results are reported in table 2 and plotted in figure 21.

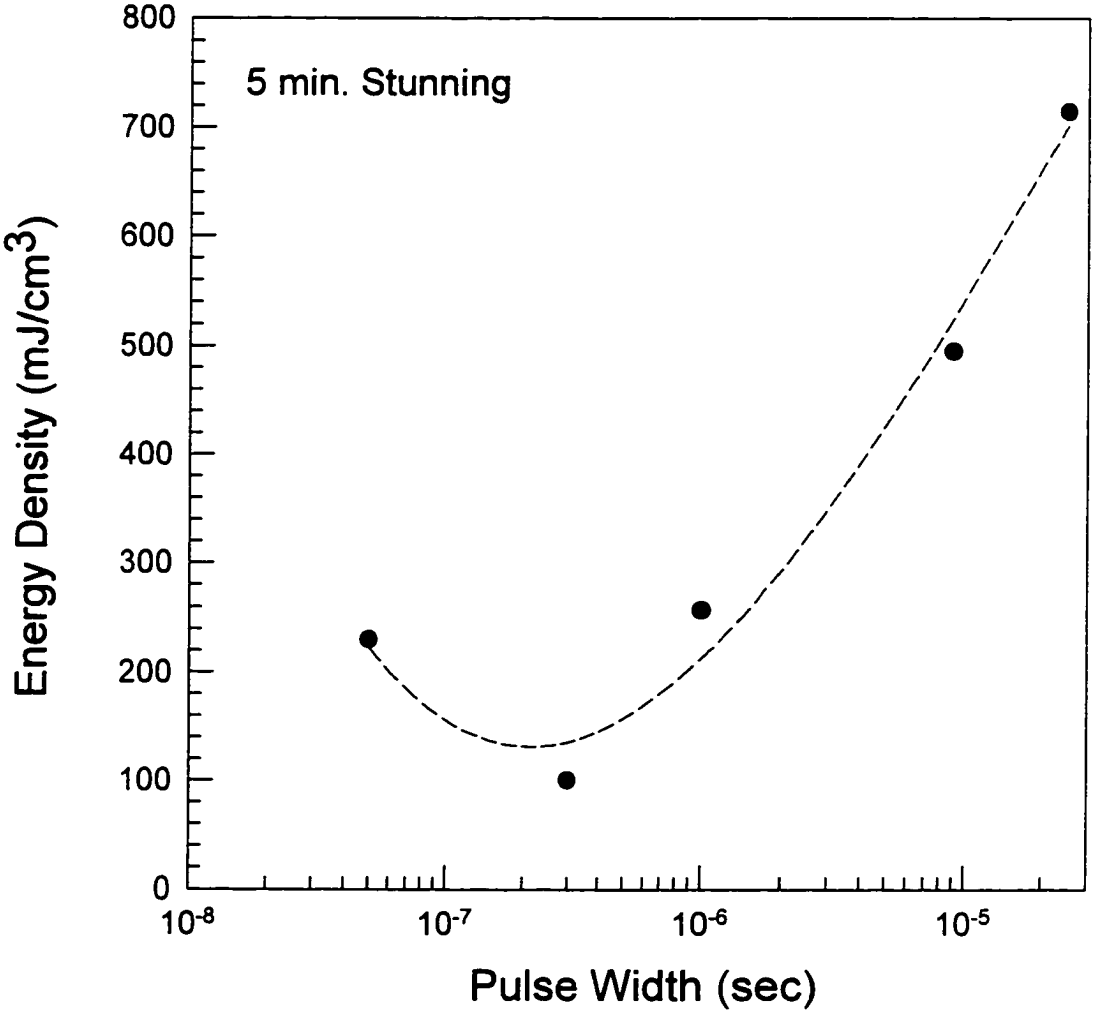

Fig. 20. Energy density expenditure versus pulse width for 5 minutes stunning duration

Table II
Results of changing field strength for different pulses

E KV/cm	300 ns Rect Pulse		1μs Rect Pulse		5 μs sin wave Pulse	
	Energy Density (mJ/cm^3)	Stunning period (min)	Energy Density (mJ/cm^3)	Stunning period (min)	Energy Density (mJ/cm^3)	Stunning period (min)
0.5	2.1	0.5	7.1	0.5	35.6	1
1	8.6	1	28.6	1.5	142.8	2.5
3	77.1	4	257	6	1285.6	15
5	214.3	8	714.3	30		
10	857.1	50	2857	120		
20	3428.4	360	11428	Mortality		

Figure 21 gave us an idea about the required electrical field strength for a certain stunning duration. For typical cooling system residence time of 10 minutes, field strength above 5 kV/cm with pulse duration of 1 μs would ensure no settlements inside the pipes. To be able to compare between different pulse shapes, table 1 data are graphed in figure 22 in terms of energy density rather than electric field. Energy density of the applied field is expressed by

$$Energy\ Density = \int_0^{\tau} \frac{E^2(t)\,dt}{\rho} \tag{4}$$

where τ is the pulse width and ρ is the suspension resistivity.

Figure 22 shows that 300 ns pulses are slightly more effective than the 1 μs pulses, and much more effective than the sine wave 5 μs pulses. This means that in the sub-microsecond range, maximum efficiency for certain stunning duration would be expected. Figures 21 and 22 show that the stunning effect is dependent on both energy density and electric field strength. It was also

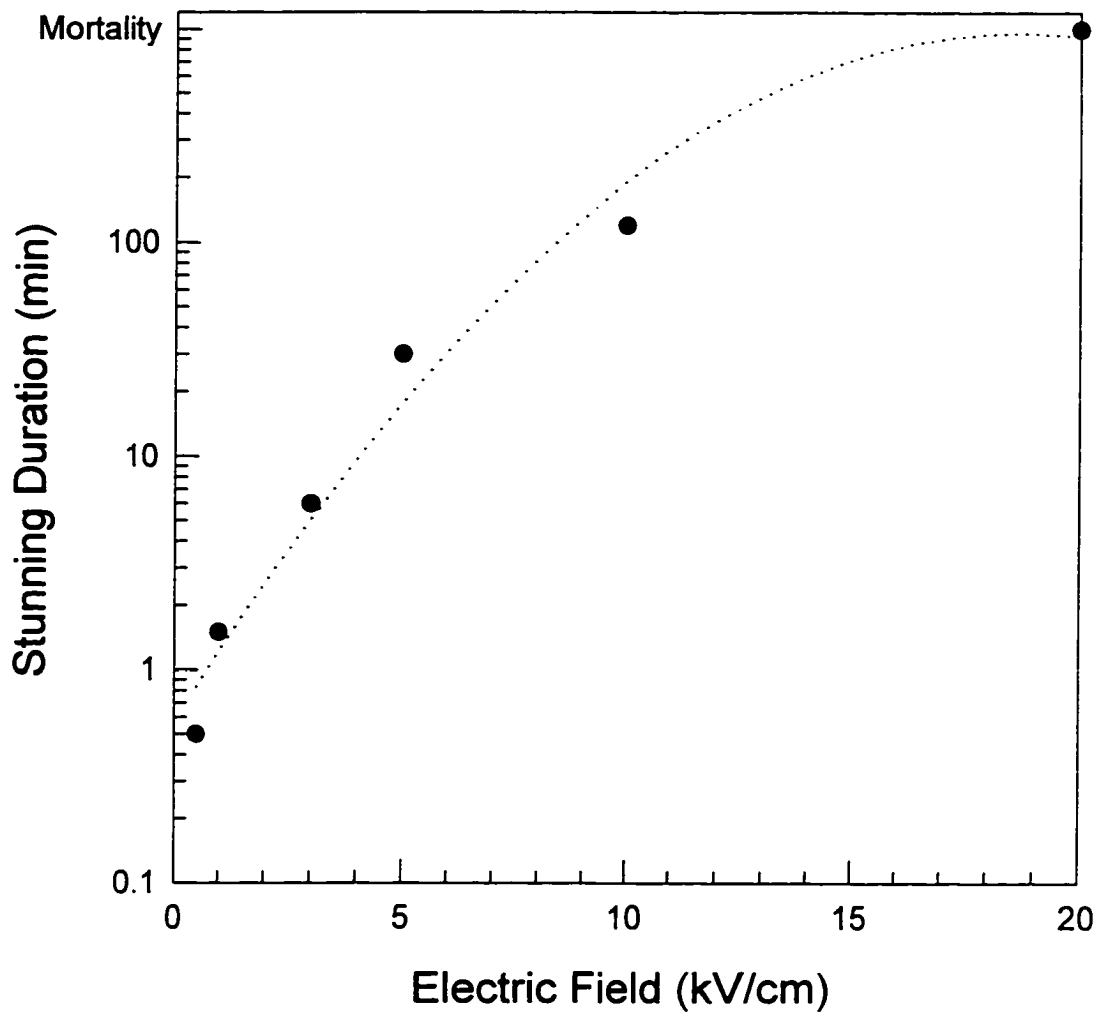

Fig. 21. Hydrozoan stunning duration versus electric field strength for 1 μs rectangular pulses

concluded from the higher effect of rectangular pulses compared to sine wave pulses, that higher frequencies of rectangular pulses are more effective than lower frequency components of sine wave pulses. Consequently, as a general statment, higher frequency components yield greater efficiency in pulses of microsecond duration. However, industrial limitations and different switch reliabilities may favor certain pulse shapes against the price of some loss in efficiency.

5.5.2 Effect of repetition rate

The effect of pulse repetition rate was investigated by applying consecutive pulses at different repetition rates and comparing the resultant effect with that of one pulse having the same total energy. A fixed electric field value of 3 kV/cm was used in these experiments. The results are shown in figure 23. It shows that one shot is more effective than burst of shots with the same energy. Moreover, faster repetition rate (20 Hz) was more efficient than a slower repetition rate (1 Hz). This means that by applying consecutive pulses with a faster rate than the rate of recovery, cumulative effects can be obtained.

This is of special interest in practical applications, because the generation of a burst of pulses with medium voltage is technically easier than the generation of a single, very high voltage pulse. In order to answer the question of how much the electric field can be reduced by applying even faster consecutive pulses and still have a desirable effect, another experiment using the MOSFET pulser was done. A fixed value of the electric field of 250 V/cm was chosen because this value represents the transition from gas tube switch generators to reliable, inexpensive semiconductor switch generators. This value was calculated by

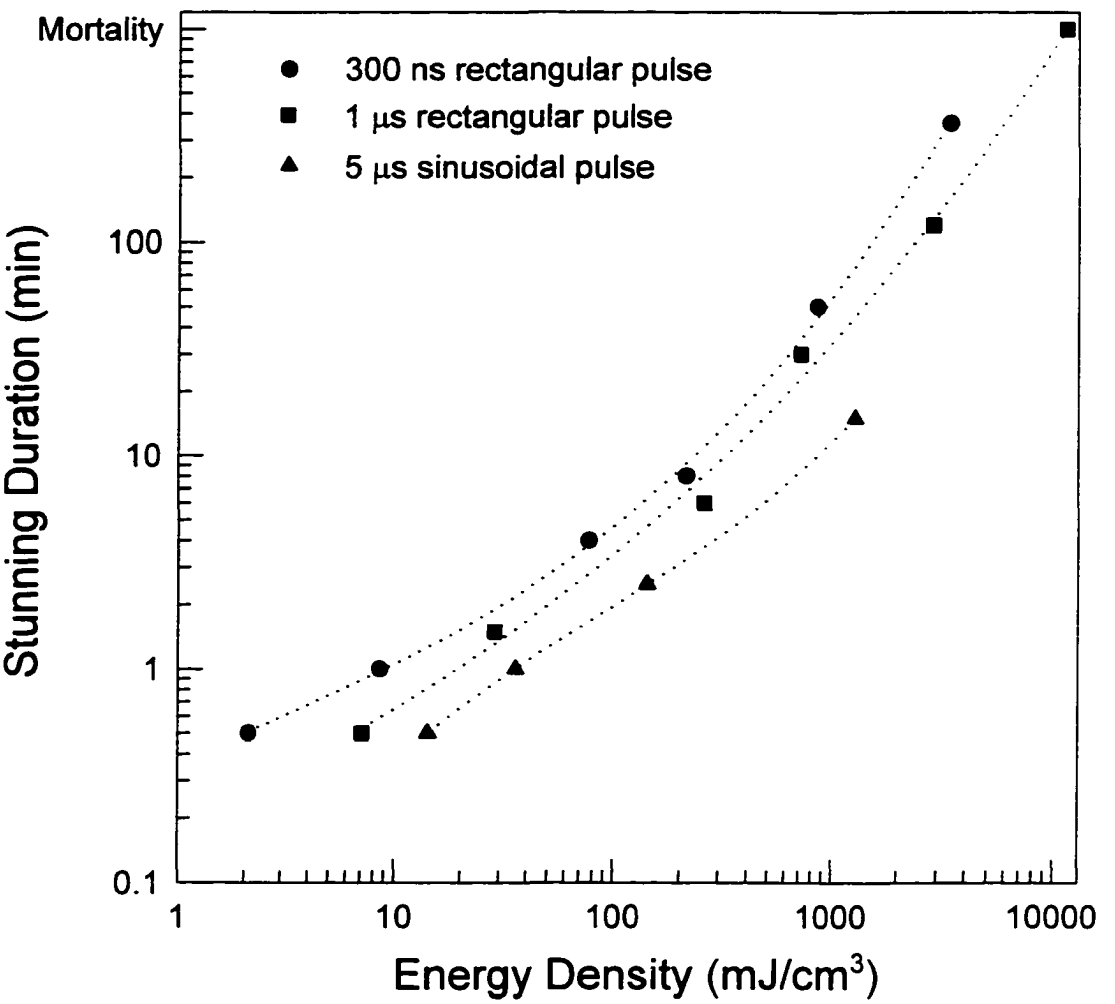

Fig. 22. Stunning duration dependence on energy density with pulse shape as parameter

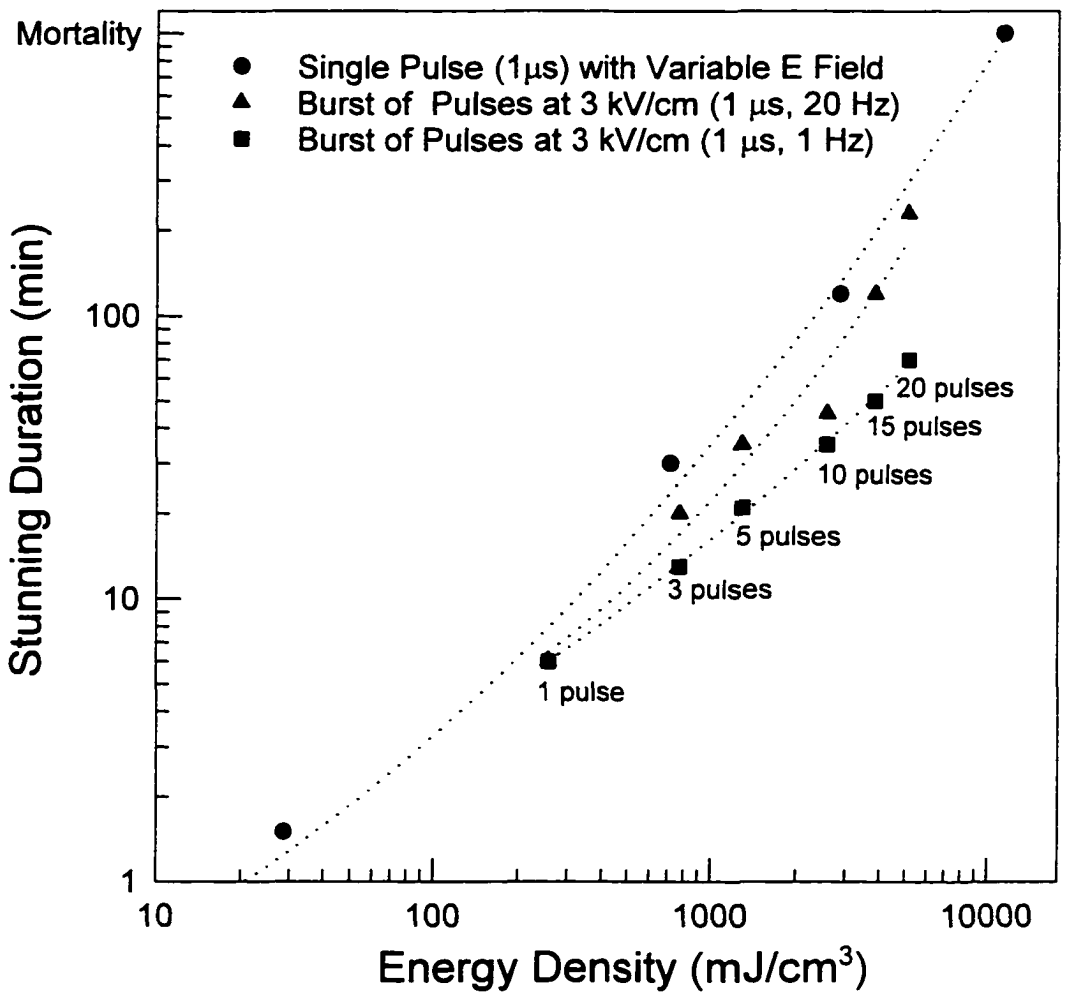

Fig. 23. The effect of repetition rate on the stunning of hydrozoan

applying a voltage of 1.2 kV (max commercial MOSFET rating) to 2" pipe yielding an electric field of approximately 250 V/cm. One thousand pulses were applied with this value of electric field at both very low frequency (1 Hz) and very high frequency (50 kHz). No stunning response was noticed in either case. However, at this low field, the hydrozoan consistently aligned its body ia a direction parallel to the electric field.

The maximum obtainable electric field with this pulser was 1 kV/cm. At this value, I applied 120 pulses at both 1 Hz and 50 Hz. No response was noticed at 1 Hz, but slow contraction and a fast (few seconds) recovery were recorded in response to the 50 Hz field. This emphasized that the frequency plays an important role in the effect of the electric field on these species.

In order to find out if faster pulses will have more cumulative effects, we increased the frequency, in nonlinear steps, up to 50 kHz. No difference was noticed between any of these cases and the 50 Hz case. Consequently, it was concluded that the effective range of frequency is between 1 Hz and 50 Hz. In order to investigate the criteria which this cumulative effect causes, Pulses with repetition rates from 1 to 50 Hz were applied in steps of 5 Hz. .Although the difference in response was easy to recognize between the 1 Hz and the 50 Hz, it was very difficult to follow the difference between successive trials due the fast recovery of the organism.

Based on these results, it was concluded that the semiconductor pulses are not candidates for the application of biofouling, at least in the near future, as

long stunning times need much higher electric fields in the cooling system pipes than can be handled by semiconductor technology.

5.5.3 Effect of electric field on feeding ability

To investigate if the electric pulses affect the organisms ability to feed, hydrozoans were pulsed with different parameters and their behavior was monitored after the recovery process was complete. The ability to feed was tested by putting a brine shrimp in the same cuvette and by recording the hunting and digesting process. All the organisms showed normal activity including those which recovered from two hours stunning duration after 15 pulses at 20 Hz and 3 kV/cm. Figure 24 shows a recovered hydrozoan catching brine shrimp after two hours of stunning. Consequently, it was concluded that once the organism recovered, it was able to feed normally.

5.5.4 Effect of electric field on late mortality

Laboratory experiments were done to investigate the effect of the electric field pulses on hydrozoan rate of growth, or eventual mortality, after their initial recovery. Four experiments with two groups of polyps were observed, a control side and a treatment side. The treatment sides were pulsed with different field strengths including parameters that led to several hours of stunning. In all cases there were no distinctive differences between the rate of growth of the controls and treatment sides. Figure 25 shows a comparison between the control side and the treatment side with no apparent difference. The treatment side was exposed to 15 pulses at 20 Hz and 3 kV/cm. Consequently, it is concluded that

the recovery process is an "all or none" process, i.e., once the organism recovers, it recovers completely its ability to feed and grow.

Fig. 24. Effect of electric field on hydrozoan feeding ability

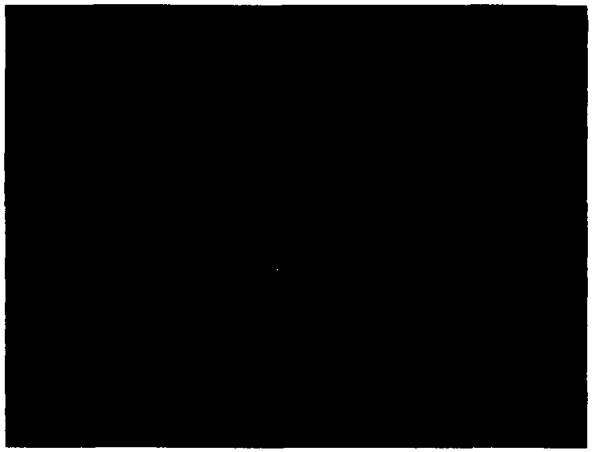

Control Side at Day 1

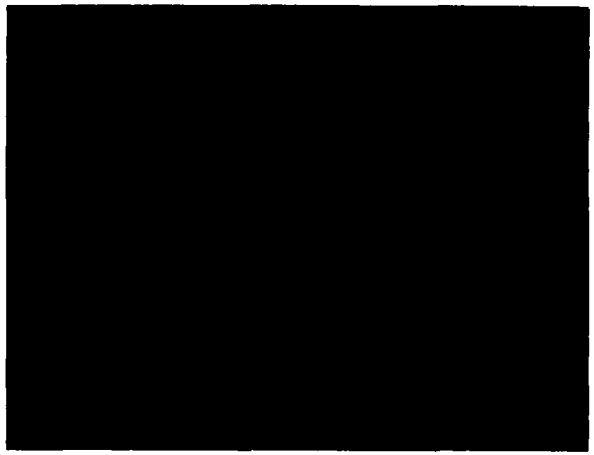

Treatment Side at Day 1 (before Pulsing)

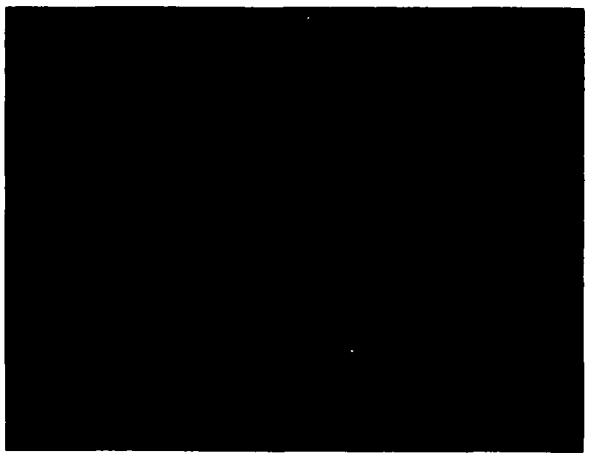

Control Side at Day 9

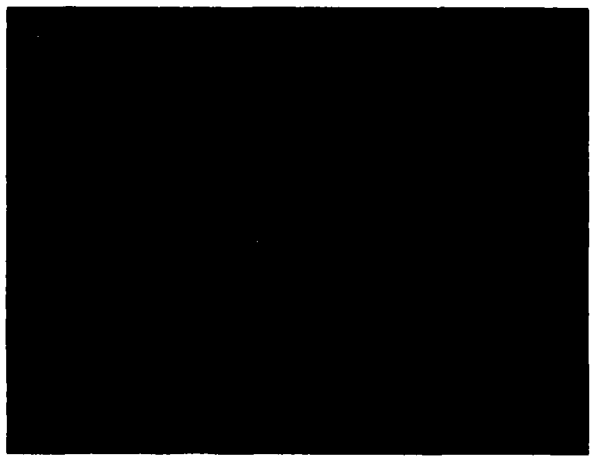

Treatment Side at Day 9

Fig. 25. Effect of electric field on late mortality

CHAPTER VI
FIELD EXPERIMENTAL WORK

6.1 Introduction

The objective of the field experiments was to demonstrate the applicability of using electric field to control biofouling in full scale systems. In these experiments, natural sea or river water was pumped through two sides, a treatment side in which the water was exposed to electric field pulses, and a control side without pulses, for comparison. Results were obtained by comparison of aquatic nuisance species settlements of the two sides. Two field experiments were performed. The first one was done in tidal water where the main fouling organisms are barnacles and hydrozoans. This experiment was located at the Elizabeth River in Chesapeake, Virginia, and was performed during the period from September, 1995 to November, 1996. The second one was conducted in fresh water where the zebra mussel is the main biofouling species. This experiment is located in River Bend nuclear power station at St. Francisville, Louisiana. It began in September 1997 and is still in progress, after collecting initial data in February 1998.

6.2 Salt Water Field Experiment

6.2.1 Experimental setup

Based on results of laboratory experiments, a large scale system was built for the field study. The pulse power generator consisted of a 50 kV constant current Maxwell power supply with an average output of 8 kW, an IAP BLT 20 kA spudo spark switch and its controller. The pulse forming network consisted of

160 high voltage capacitors 2 nF each connected in a Blumlein configuration. This configuration enabled load voltage equal to the supply voltage. The PFN was placed in transformer oil to reduce the chances of corona discharges, which could damage the system or detrimentally affect the pulse characteristics. The electrical system delivered its output pulse to two electrodes of flow through cell in which the water flows. Electrode material was of interest since the system would be expected to work in the vicinity of 10 Hz for several months before requiring maintenance or replacement. Several electrode metals including copper, steel, stainless steel, aluminum, and titanium were tested during the initial parameter configuration. With the exception of titanium, all metals displayed evidence of degradation after a short pulsing time. Electrodes constructed from titanium showed no signs of reactivity after several thousand pulses; therefore titanium was selected as the material from which to construct the electrodes.

The hydraulic portion of the system, supplied and constructed by the Applied Marine Research Laboratories (AMRL), consisted of 15 feet long biofouling observation pipes for both control and treatment sides, control and treatment distribution mainfolds, flow calibration and bypass valves, and flow through cell which had the electrodes connected to the pulse generator. A computer and controlling software was installed to monitor and record pulse characteristics and water flow. Software was also developed and installed to alert laboratory personnel via modem in the event of system failure. A steamship container was provided by Norshipco, Berkely. This container was modified and

outfitted by Norshipco according to the specification of the PERI and AMRL, and was used as a field laboratory to house the experimental apparatus. This field laboratory was placed on the end of pier 5 at the Norshipco Berkley shipyard. Figures 26 and 27 show a schematic diagram of the field system and the physical layout respectively.

6.2.2 First salt water field trial

6.2.2.1 objective

The objective of this experiment was to verify the concept of biofouling prevention with pulsed electric field in large scale field systems. The first trial of the field system began on September 1, 1995.

6.2.2.2 procedure

The field strength of the system was 12 kV/cm, with pulse duration of 770 ns, and pulse repetition rate of 20 Hz. The electrode gap was 1 cm and electrode length and width were 5 cm and 1 cm respectively. The flow rate of water through the treatment and control electrodes was adjusted using ball valves to ensure that each volume of water passing through the electrodes was exposed to at least one pulse. The approximate flow rate through the treatment and control cells was 6 L/min. This resulted in a linear velocity through the observation pipes of approximately 100 cm/sec., and a residence time in both the control and treatment sides of approximately 25 seconds. Constraints of laboratory space prohibited system designs with longer retention times.

Several components of the system failed during continuous operation. System failure was due to both intrinsic and extrinsic factors, such as rainwater

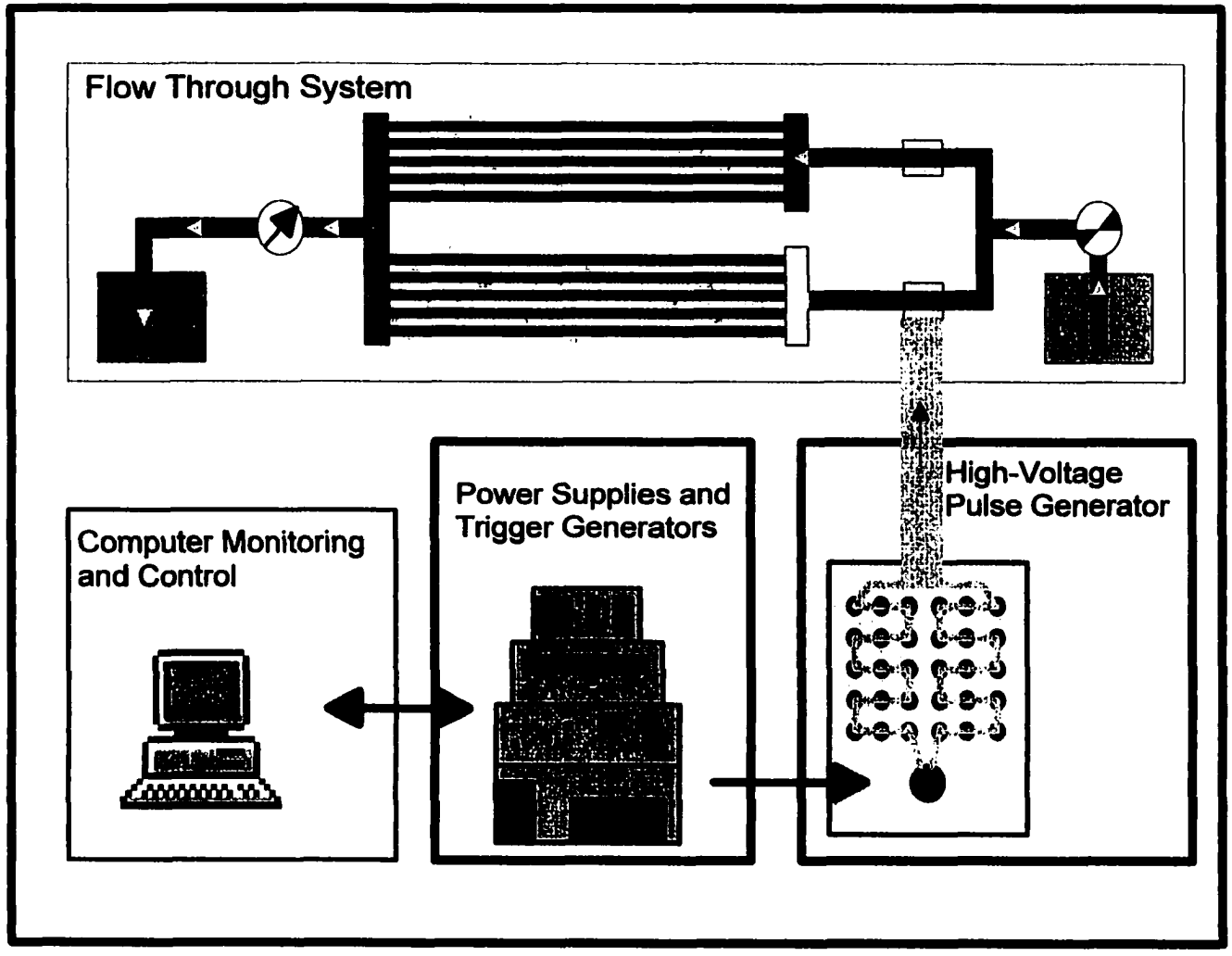

Fig. 26. Schematic diagram for the salt water field setup

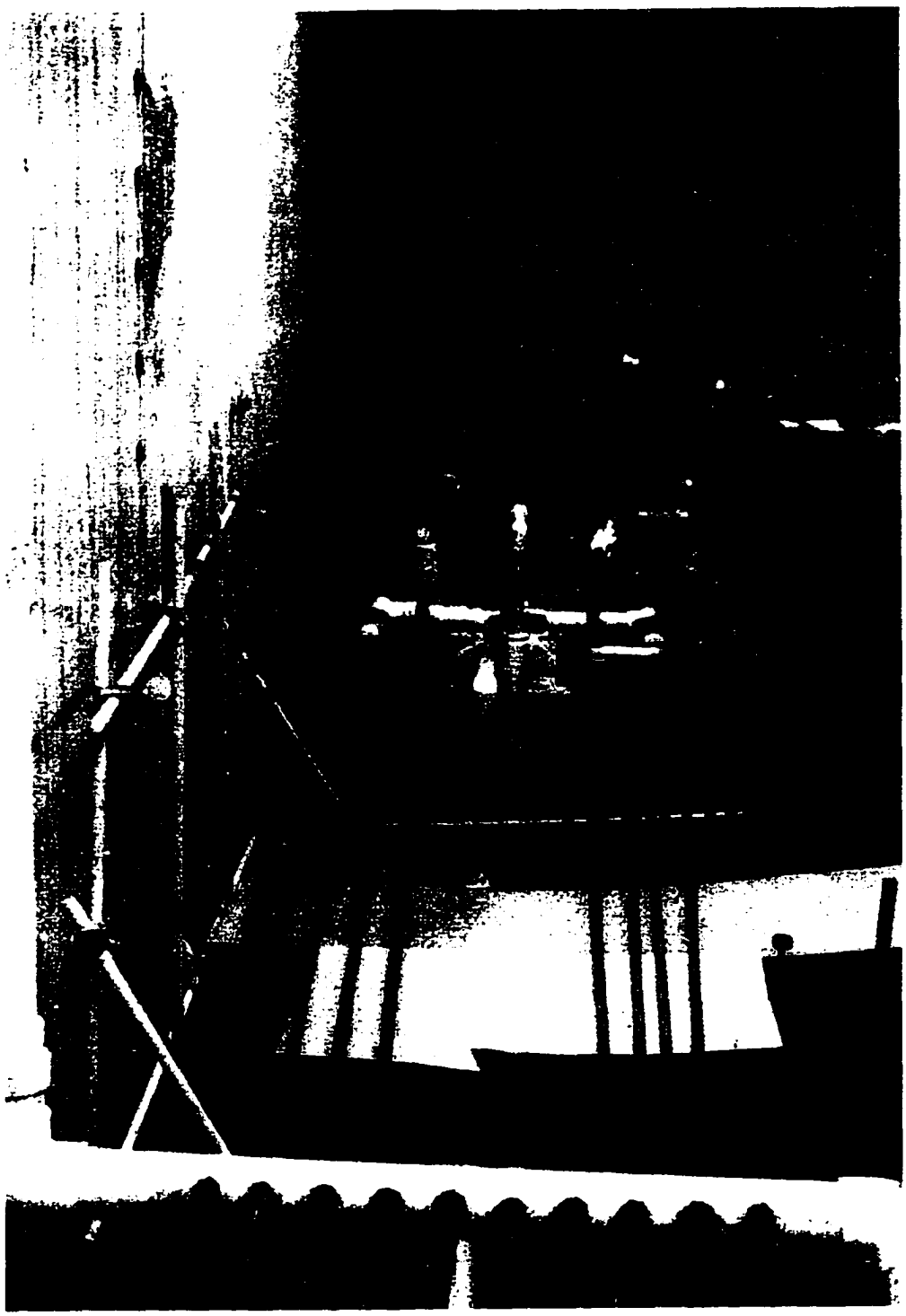

Fig. 27. Physical layout of the salt water field setup

leaking through the roof of the container, component malfunction due to overheating, dissolution of power wire shielding in the PFN oil tank, power supply fluctuations, and fouling of the water pump which supplies the experimental system with test water. These factors resulted in a premature termination of the first test.

6.2.2.3 results of the first salt water field trial

In spite of these system shutdowns, when the trial was terminated on September 19th, a quantitative visible difference in control versus treatment tubes was evident. Macroscopic fouling organisms consisted primarily of barnacles, hydrozoans, tunicates, and polychaete worms, and were three times more abundant on the control observation tubes than on the treatment tubes. This was particularly impressive, since the treatment tubes were exposed to untreated water for approximately 25% of the trial duration as a result of system malfunction.

6.2.3 Second salt water field trial

6.2.3.1 objective

The objective of this trial was to continue the effort of the first one avoiding the past difficulties.

6.2.3.2 procedure

Adjustments, modifications, and replacement of some system components, as well as repairs to the field laboratory roof, were performed. Replaced components include the support and trigger system for the switch, as well as the BLT spudo spark switch, which was replaced by a 260 MW EG&G

thyratron. These modifications resulted in longer and more consistent operation of the pulse system. The modified system was started on October 30, 1995. The system ran uninterrupted for 20 days, at which point the trial was terminated due to switch failure. Due to scheduling difficulties, the system continued to pump untreated water through the treatment cell for an additional two days.

6.2.3.3 results of the second salt water field trial

An examination of the thyratron switch, and consultation with the manufacturer suggested that the premature failure of the switch was likely due to changes in water salinity, which caused fluctuations in the water resistivity, and consequently a mismatch occurred between the pulse power system and the load. In such a case, part of the power flow directed into the water is reflected back into the power system and can cause damage, particularly at the switch.

Approximately 1100 total animals were observed when the control tubes were flushed, of which approximately 600 were barnacles, with hydrozoans, polycheate worms, and tunicates comprising the rest of the total. The only organisms observed on the treatment tubes were extremely small. The size of the organisms was consistent with animals that had colonized within the last two days of the experiment, when the water flowed through the system untreated. Therefore, it was concluded that the pulse configuration and apparatus was 100% effective in preventing biofouling. During 20 days of operation, the switch fired 35 million shots and treated 48,000 gallons of water at a cost in electricity of $10.70, or $1 for each 4800 gallons of water.

6.2.4 Third salt water field trial

6.2.4.1 Objective

Since the results from the previous trials using a 12 kV/cm system demonstrated 100% effectiveness in preventing biofouling, a subsequent trial was initiated in May 1996 to test the effectiveness of the system at approximately half the initial power.

6.2.4.2 procedure

The electrode gap was increased to 2 cm, and the electrode length and width were changed to 5 and 2.6 cm respectively. The voltage was slightly higher compared to the first test series to compensate for the mismatch of the load, and the electric field in the water was 6.45 kV/cm, with a pulse duration of 770 nsec, and a repetition rate of 12 Hz. The flow rate was increased to 4 gal/min due to the larger volume treated per pulse as a result of the increased electrode cell volume. To insure adequate water supply to the field system, a second pump was placed in parallel with the first supply pump. The trial was terminated after 23 days without component malfunction.

6.2.4.3 results of the third salt water field trial

While the number of animals observed on the control side were considerably less than those observed in the first trial, no animals were found on the treatment side. Table 3 shows the results of this trial and figure 28 shows the physical results where the treatment tubes can be seen to be clear of biofouling versus the fouled control side. A total of 132,000 gallons was treated over the duration of the experiment at an expenditure of approximately $11 in electricity.

A powdery buildup was observed on the relatively large anode at the end of the run. An X-ray diffraction analysis revealed the composition of the

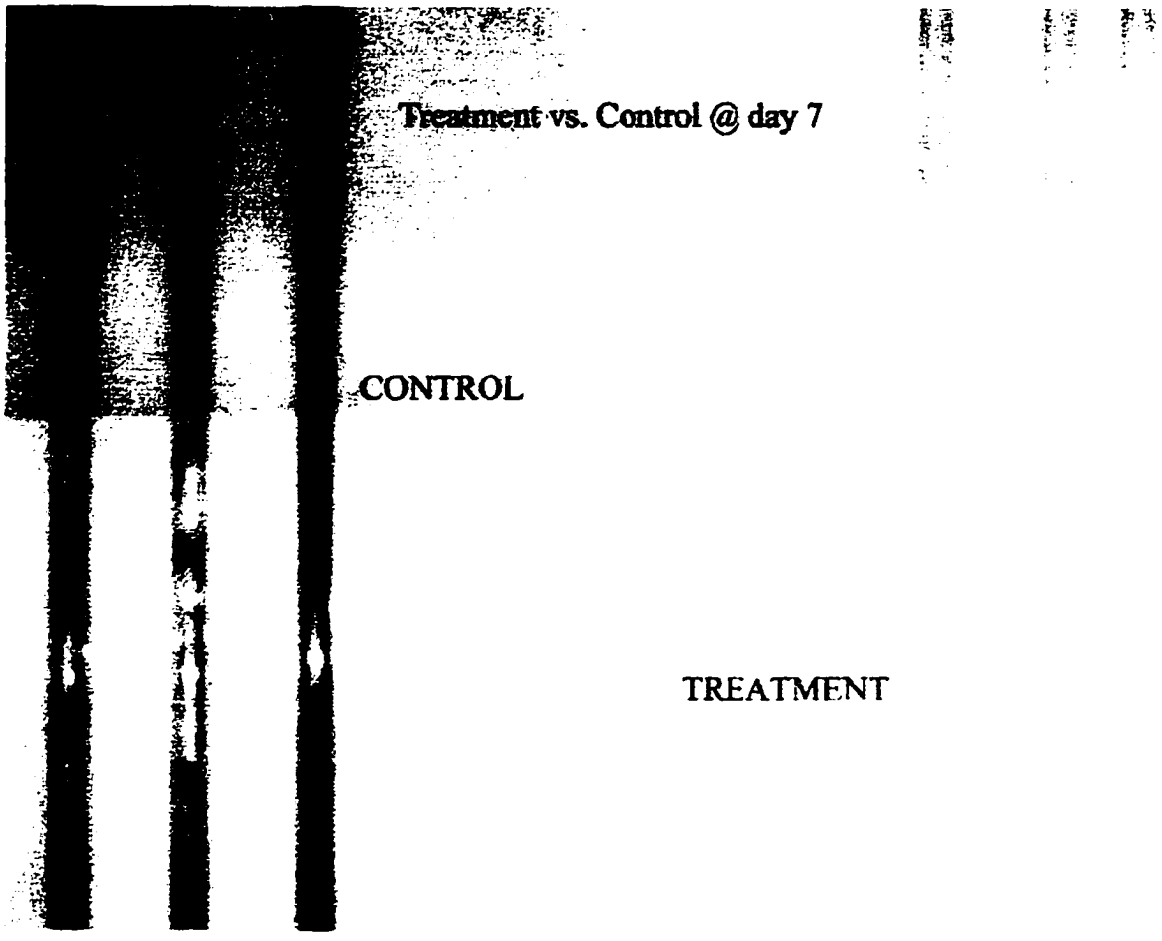

Fig. 28. Physical results of the third salt water field trial

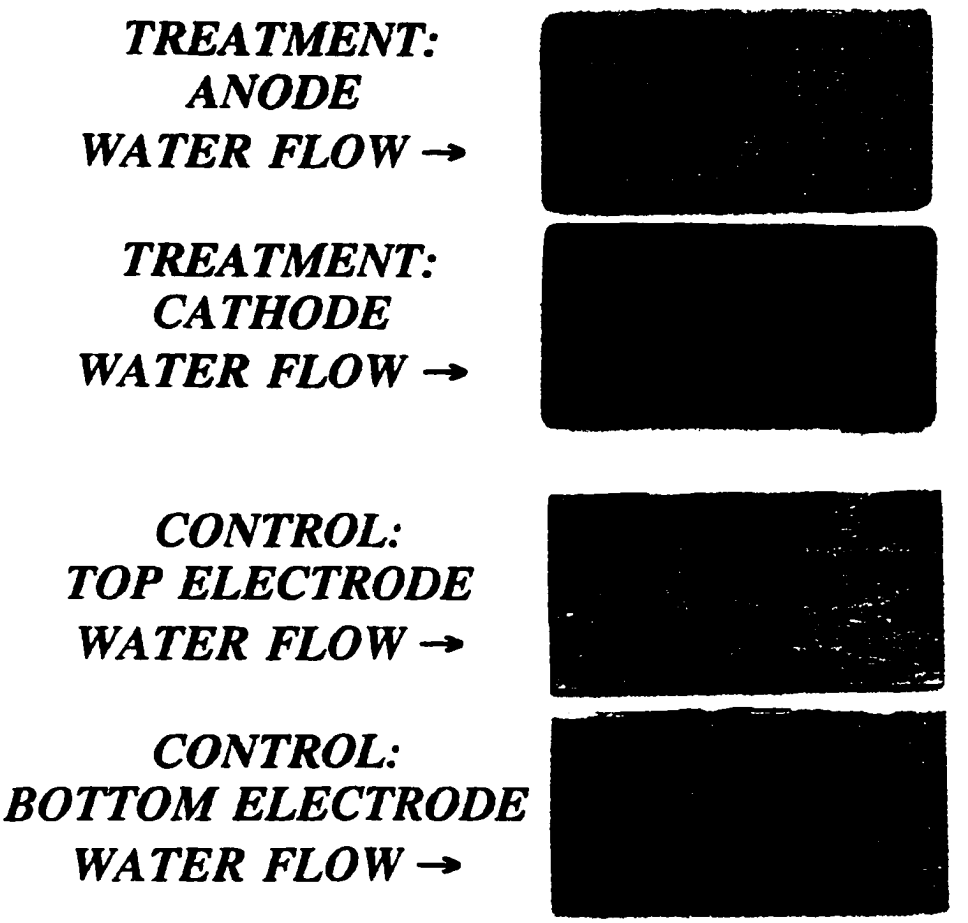

Fig. 29. Picture of control and treatment electrodes after the third salt water field trial

substance to be titanium dioxide. Figure 29 pictures the treatment and the control electrodes after the second trial.

Table III
Results of the third salt water field trial

Taxo	Control	Treatment (6.45 kV/cm)
Barnacles	14	0
Tunicates	19	0
Polychaetes	3	0
Hydrozoans	8	0
Mussels	15	0

6.2.5 Fourth salt water field trial

6.2.5.1 objective

Because the previous trial, performed at 6.45 kV/cm, 770 nsec pulse duration appeared to be completely effective at biofouling prevention, it was decided to proceed with field strength reduction in an attempt to determine the minimum operating threshold, or the maximum efficiency parameters.

6.2.5.2 procedure

In order to test the effect of the three different electric field intensities simultaneously, three treatment cells connected in series were constructed at the treatment side instead of one cell. In order to match the impedance of the Blumlein pulse forming network, a dummy cell was added in parallel with the three cells. This setup is shown in figure 30. This system yielded treatments of 3 kV/cm, 1.5 kV/cm, and 0.75 kV/cm field intensities. All treatment pulse duration was 770 nsec, at a frequency of 10 Hz.

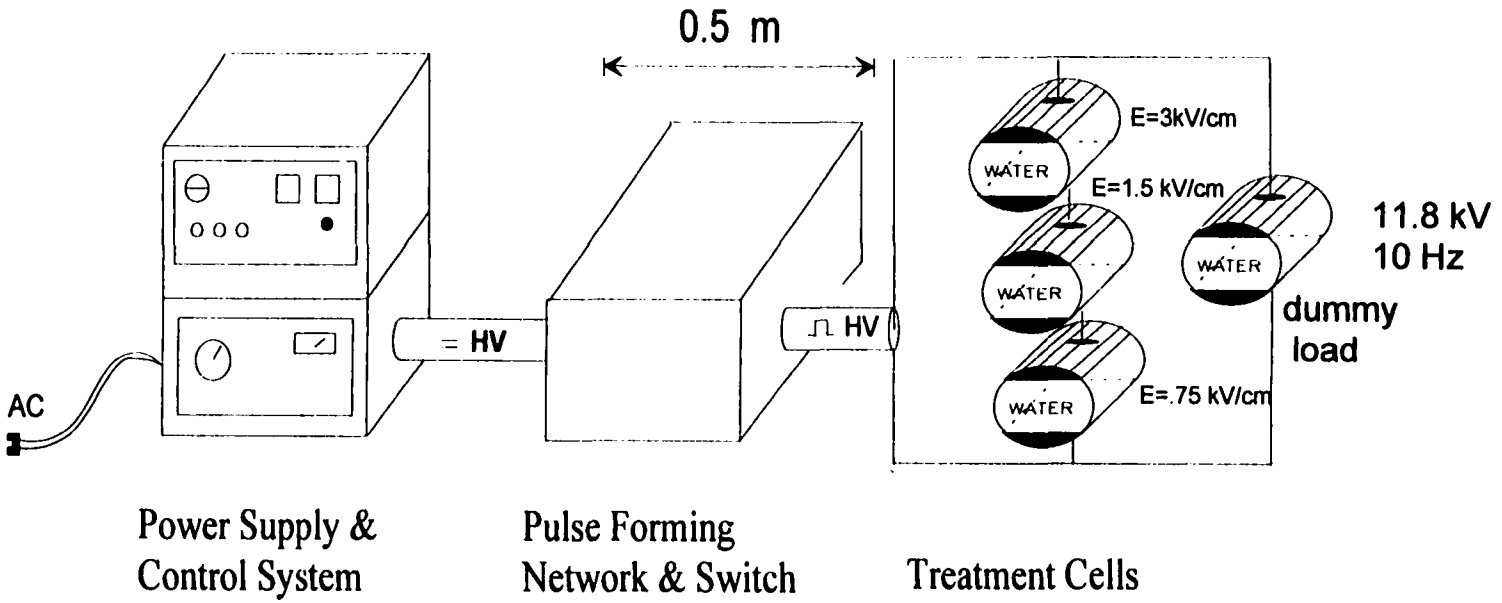

Fig. 30. Schematic diagram for the fourth salt water trial setup

Because of the increased number of treatments and the dummy cell, the number of supply pumps was increased to four, placed in parallel. The test was initiated on September 25, 1996, and ran for 13 days , but was repeatedly subjected to power interruptions due to shipyard activity. Because telephone lines had not been reinstalled in the field lab, the system could not be monitored or remotely controlled. Thus, when the power was interrupted and then restored, the supply pumps started, but the pulse generator did not. This situation resulted in exposure of the treatment observation tubes to untreated water on several occasions. When the power was permanently disconnected by the shipyard to accommodate an incoming ship, the trial was terminated.

6.2.5.3 results of the fourth salt water field trial

In spite of several interruptions, the treated tubes were substantially less fouled than the controls in terms of barnacles. Table 4 tabulates these results.

Table IV
Results of the fourth salt water field trial

Taxa	3 kV/cm	1.5 kV/cm	0.75 kV/cm	Control
Barnacles	1	1	5	69
Tunicates	3	4	2	0
Worms	0	0	0	1
Hydrozoans	0	2	0	4

6.2.6 Fifth salt water field trial

6.2.6.1 objective

Although it was difficult to interpret the results of the September/October trial, it was decided to continue lowering the field intensity, to determine whether effective control of biofouling was possible at sub-kV/cm intensities.

6.2.6.2 procedure

The field laboratory was relocated to a site with secure power and telephone service to ensure that there would be no power or communication/control system interruptions during the trial. The system was reconfigured by putting the PFN into a cascaded configuration to give a pulse width of 4 μs, and the field strengths were lowered to 800, 400, and 200 V/cm. This modification necessitated reducing the pulse frequency to 5 Hz in order to give the thyratron enough time to recover between pulses and avoid conduction locking. The treatment cells from the previous 13 days trial were reused. This final trial was initiated on November 6, 1996, and ran through the 26th of November.

6.2.6.3 results of the fifth salt water field trial

Counts of observed macro organisms are reported in table 5.

Table V
Results of the fifth salt water field trial

Taxo	800 V/cm	400 V/cm	200 V/cm	Control
Barnacles	10	10	8	19
Tunicates	1	1	1	0
Worms	0	0	0	0
Hydrozoans	0	0	1	2

A summary of the salt water field experiments is plotted in figure 31 in terms of electric field strength versus biofouling prevention efficiency for barnacles. Efficiency was calculated by quantitative comparison of control side and treatment side.

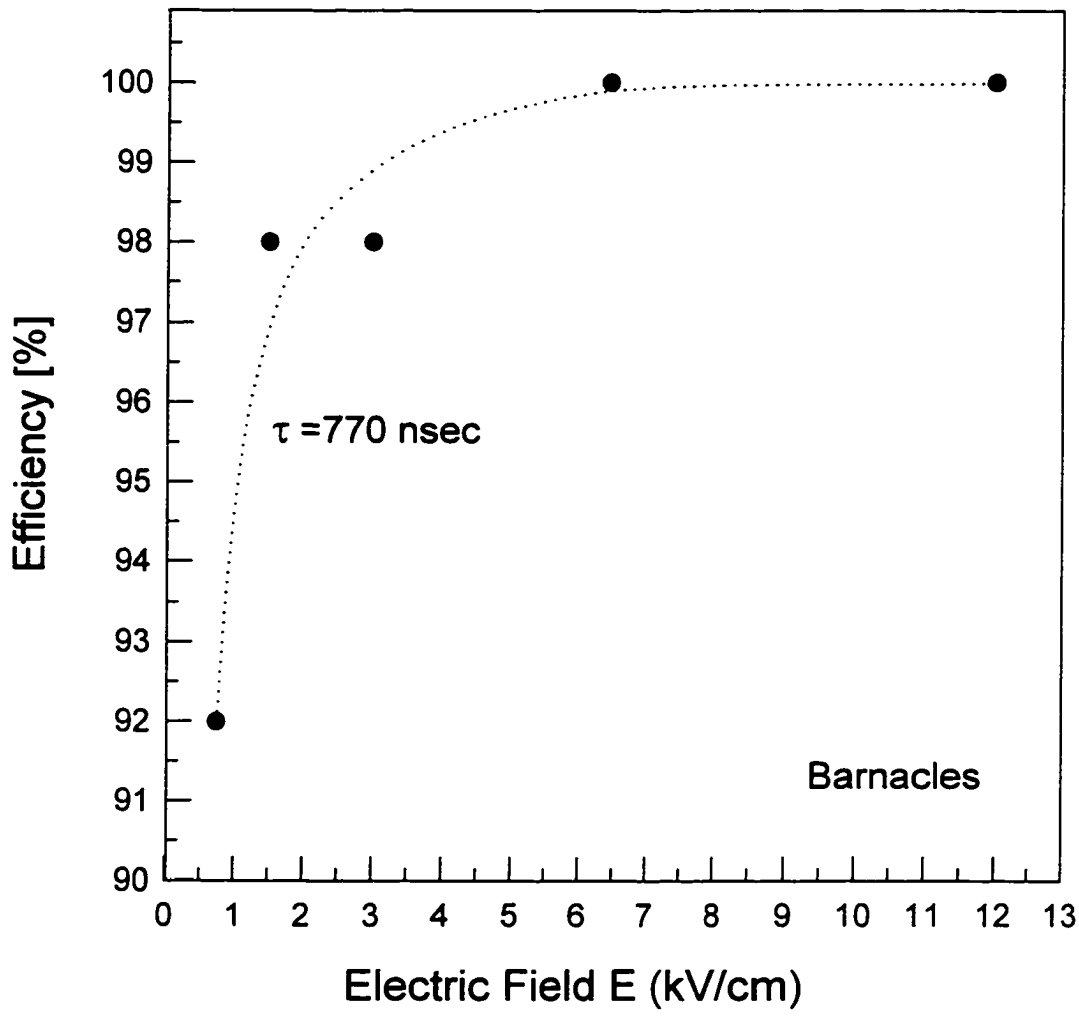

Fig. 31. Biofouling prevention efficiency versus electric field for salt water field trials

6.3 Fresh Water Field Experiment

River Bend Nuclear Power Station, in St. Francisville, Louisiana, was selected as the study site. The plant withdraws make-up water for cooling towers from the Mississippi River which is infested with zebra mussels. The make-up water passes through clarifiers prior to entering the cooling tower conduits. Multi-year monitoring by plant personnel indicated that the mussels were consistently found in the spring and fall, with peak densities occurring in October. The study was originally to be conducted between September and November of 1997. It has, however been extended to at least June of 1998. This study had three main objectives:

1) To determine if the pulsed field affected planktonic mussel behavior after exposure to the field or caused mortalities in these early life stages and, as reasonable, document effects on other entrained species.

(2) To determine the pulsed field's post-exposure effects on mussel settlement and, as reasonable, on other macrofouling species such as bryozoa.

(3) To determine qualitatively if electrode scaling noted in previous studies could be eliminated or reduced by alternating polarities of the electrical system.

6.3.1 Experimental setup

Test setup design generally followed the design used in previous macrofouling control studies. The hydraulic portion of the River Bend test setup (designed and built by the crew of Acre International Corp.) was designed to be constructed primarily of two inch PVC pipe. It was discovered, only after the field crew arrived on site, that the point of raw water access, designed by plant

personnel, was through a 3/4 inch stainless tap and, as the plant is a nuclear facility, it was impossible to move to a larger tap on short notice. So, pressurized raw water traveled through the plant's three inch stainless service water piping and to the 3/4 inch tap. The two inch test setup header was connected to this tap. Beyond the tap, water flowed through an in-line, 275 gallon flow-control tank, an in-line pump, several control valves. The header was fitted with a pressure gauge. Flow from the header was split and directed into a control side and a treatment side. Flows into the two sides were equalized using multiple control valves installed in each side. Pressure gauges were also installed in each side. A pulsed electric field was generated in an in-line test cell in the treatment side. The two inch PVC control and treatment sides discharged into separate bioboxes. The bioboxes were epoxy-coated rectangular steel tanks approximately 2.5 feet wide, 2.5 feet high and 4.5 feet long. The useable volume of the tanks was nominally 150 gallons each. The treatment and control PVC piping entering the tanks was plumbed to prevent siphoning, and tank discharge ports were near the top of the tanks, such that should flow stop the tanks would not be de-watered. The inlet was at one end of a tank, the discharge at the other. Each biobox tank held four, two foot square by 1/4 inch thick PVC settlement plates. The four plates were spaced equidistant from each other, alternatively placed against the left or right sides, and on the bottom of their respective tanks to channels the flow. Veligers in the treatment tank, adjacent to the plate nearest inlet, should have had the shortest time to recover after electric treatment, those

at the discharge end the longest recovery time. Overflow from the bioboxes was discharged to the clarifier pit.

A flow-through electric test cell was mounted in the two inch PVC treatment side of the test stand just prior to entry into the treatment biobox. The cell body was clear plexiglass approximately 60 X 5 X 5 cm. Located inside the cell were two titanium electrodes (4 X 4 X 15 cm plates) The electrodes were centrally located on opposing walls of the cell. Metal conductors extended through the plexiglass walls from each plate and provided studs for electrical connections. A three quarter inch diameter tap was placed in the PVC pipe between the flow through cell and the treatment biobox to provide a port from which to withdraw treated water and observe the effects on planktonic mussels. A similar tap was also placed in the control side of the test stand.

Each volume of water in the treatment side was designed to be pulsed by at least two 5μs pulses of different polarities to prevent electrode scaling noted in previous freshwater studies. These pulses were provided from a Megapulse, Inc. pulse generator, which had been used for twenty years in Loran-C transmitting systems and has demonstrated high efficiency and reliability. This pulser was made from "off the shelf components", so it was much bigger and heavier from what would be designed for the purpose of biofouling prevention. A flow switch was inserted in the treatment water line to disconnect the pulse generator in case the water flow stopped, so that the system does not arc due to existence of air between the electrodes. The signal to the electrodes was constantly monitored using a Tektronix's oscilloscope and routinely interrogated via modem to Physical

Electronics Research laboratories in Norfolk, VA, and to Megapulse's facilities in Bedford, MA. Water flow In the system was monitored by Entergy's environmental personnel stationed on site. Monitoring efforts were coordinated by Acres International's scientists, in Amherst, NY. Figures 32 and 33 show a schematic diagram and the physical layout of the system setup respectively.

6.3.2 First fresh water field trial

Preliminary studies showed that a value of 5 kV/cm for the electric field will be efficient for inhibiting mussel attachments. The scheduled time for the experiment was September 1997, which is the high season for veligers. Due to an unplanned extension and a River Bend plant outage, the test setup was not completed until October 14, 1997. Flow problems, which required on-site piping modifications to the original design, further delayed initiation of the test until November 1. Although the study was not started until November 1, river temperatures remained suitable for veliger tests. The test site was visited on January 29 for preliminary results, and the system was shut off until the spring trial.

6.3.2.1 procedure

Setup modifications included the 275 gallon flow control tank. The tank was required to remove in-line gasses (bubbles) created by compression/expansion that occurred as water passed between the 3/4 inch to the two inch PVC lines. Although the bubble problem was solved, the modifications meant the test setup could deliver approximately 25 to 30 GPM (or

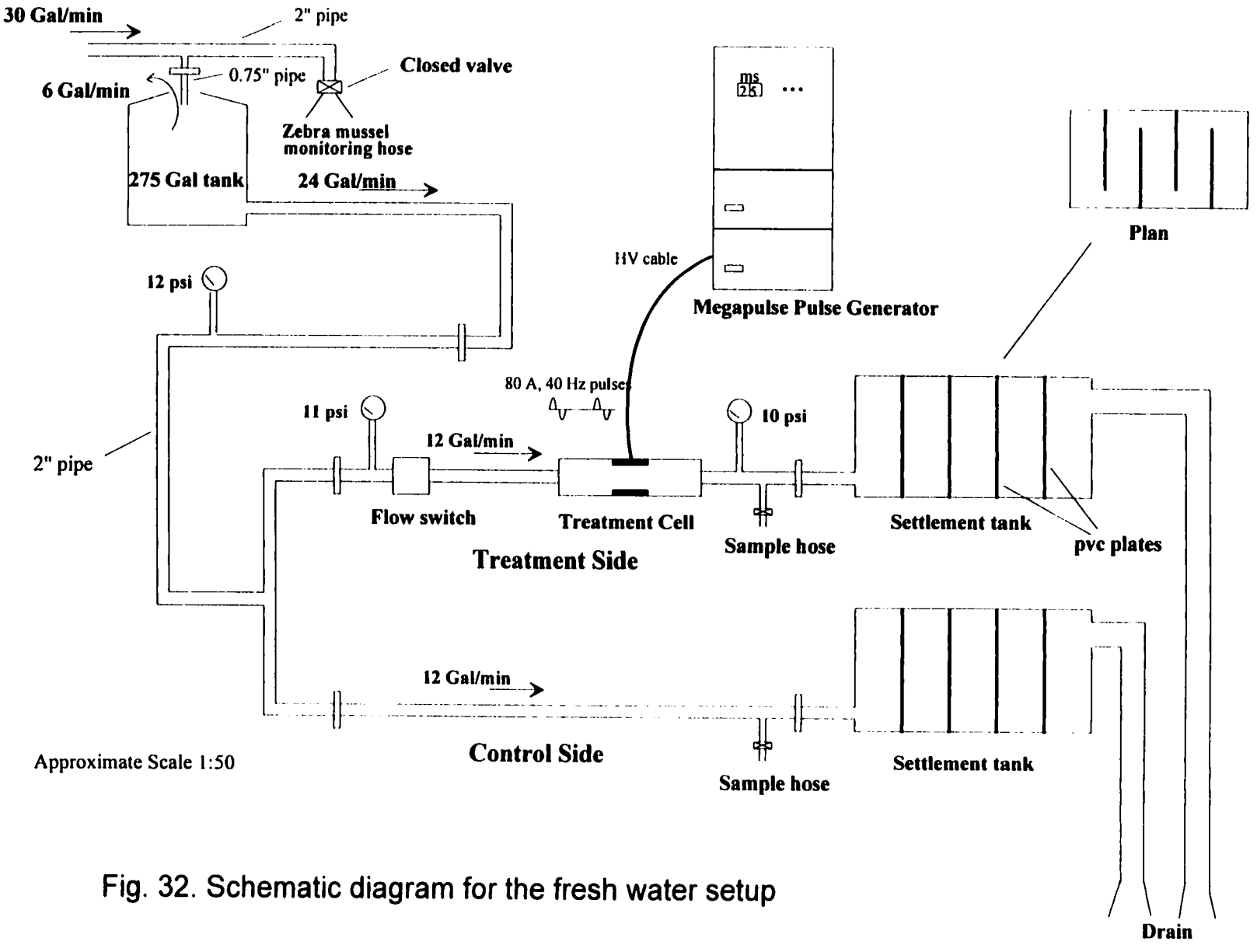

Fig. 32. Schematic diagram for the fresh water setup

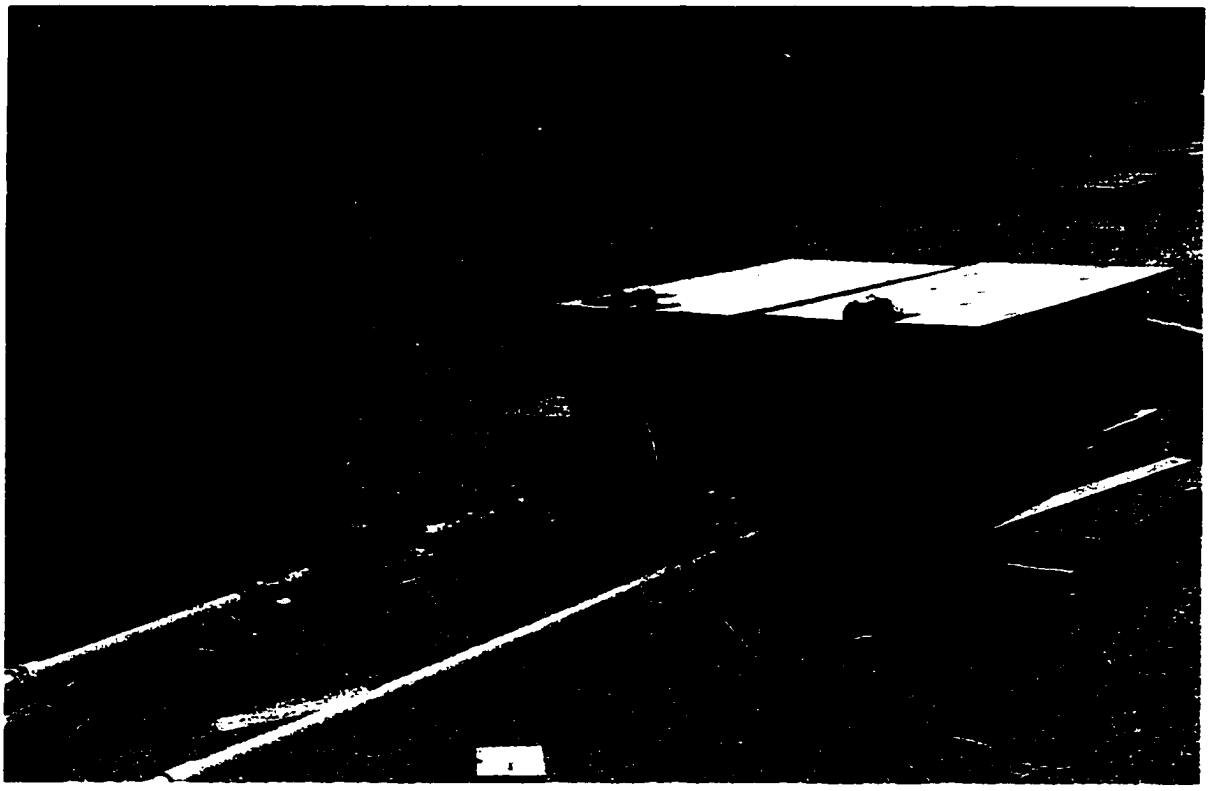

Fig. 33. Physical layout of the fresh water setup

~15 GPM/side) rather than the 50 GPM/side as was intended. The flow to the tanks was interrupted on two occasions. Once Plant Operations had to shut the system off to prevent flooding of the clarifier pit, and on the other occasion snake, fish and frog parts clogged the 3/4 inch tap.

The system was designed to have 200 Ω load resistance. Consequently a maximum current of 100 A would have yielded a load voltage of 20 kV and an electric field of 5 kV/cm between the 4 cm electrode gap. Due to the delay in the start of the trial (from September to November), the water resistivity changed from 3000 Ω.cm to 2200 Ω.cm which resulted in a decrease of the load resistance from 200 Ω to 150 Ω. As a result, the load voltage was 15 kV, corresponding to an electric field of 3.75 kV/cm. To compensate for this drop in electric field, the frequency was raised from 6 Hz to 40 Hz. At this frequency each volume of water was pulsed 13 times. The pulsed power delivered to the cell averaged over the pulse duration of 5 μs was 0.75 MW. The average dc power was 300 W. Assuming that it will be possible to keep the tubes completely free of biofouling at these power levels (which needs to be shown in the upcoming trials), the treatment cost would be $55/day for a service water rate of 1,000 GPM. This cost could possibly be further decreased by optimizing the field parameters and number of shots per volume of water.

6.3.2.2 results of the first fresh water trial

On November 2 as test samples were collected river water temperatures were > 60 degrees Fahrenheit and veligers were observed. However, due to a temporary alteration in the operation of plant clarifiers, chlorine was entering the

study apparatus on November 1. The chlorine injection point was quickly re-routed, downstream of the study raw-water tap. Chlorine residuals, although abated, precluded collection of useful veliger behavior data related to the electric field study in November. Moreover, veligers were not found on the Jan 29-Feb 3 site visit and so the effects of the pulsed field on veliger behavior and mortalities could not be determined. It is anticipated veliger data will be obtained during a July, 1998 site visit.

On January 29, after the system had been in operation for approximately three months, scaling, which had been a concern in studies conducted on Lake Ontario [21], could not be observed on either electrode of the test cell. Water quality data (total hardness as $CaCO_3$) for the lower Mississippi River at Luling, LA [12] where scaling occurred in previous studies was compared. The comparison indicated that $CaCO_3$ concentrations were similar at both sites (~130mg/l) although maximum concentrations at Luling were higher at 150 mg/l. This would suggest the lack of scaling at River Bend cannot be attributed to low calcium levels in the Mississippi River. The study data suggests that the alternating polarities generated by the Megapulse power supply (before and after December 1^{st}) reduced or eliminated the scaling problem noted in the Lake Ontario studies.

To evaluate settlement density, the PVC plates were removed from the tanks and the upstream and downstream surfaces of each plate scraped, separately, into a nominal 40 micrometer USGS sieve. The filtrate was placed into separate sample bottles on which was noted the surface scraped and plate

position in a tank. The samples were preserved with isopropyl alcohol and returned to Acres laboratory for analysis. Settlement densities were based on the area of the plates that were continually immersed. Mussel settlement density on the PVC control plates was 7/m2 , while that on the treatment plates was only 0.5/m2 (13 and 1 mussel respectively), suggesting an approximate control efficiency of 93 percent. The settlement densities on the control plates, however, were very low in the River Bend study probably because of the late field start. Densities were too low to evaluate variations in mussel density versus plate position in the tank. The low densities, the limited interruptions in flow, and the loss of the positive voltage spike confounded the analysis of data.

CHAPTER VII
CONCLUSIONS

Clinical and theoretical evidence indicate that electric fields have biological effects. These effects can range from recoverable disturbance to mortality induction depending on the field parameters and time of exposure. The mechanism of electric field interaction with biological systems has been well identified and analyzed at the cellular level; however, the analysis of this interaction is relatively undeveloped at macroscopic levels due to the high complexity of these biological systems. Consequently, experimental work is the tool to demonstrate and further investigate these effects. In this thesis, the effect of pulsed electric fields on aquatic nuisance species was investigated. The effects of different pulse parameters on the stunning duration were investigated via laboratory experiments. These parameters included pulse width, pulse amplitude, pulse shape, and pulse repetition rate. These parameters were optimized to determine a stunning duration long enough for hydrozoans to be flushed from marine cooling systems without gripping pipe walls. Validation of the electric field as a biofouling control method was demonstrated via two field experiments designed using these optimized parameters.

Laboratory experiments showed that the minimum stimulating field for hydrozoans is 0.5 kV/cm at 0.3 μs pulse width. This field resulted in 0.5 minute stunning duration. At the other extreme, the minimum field that can cause electrocution is 20 kV/cm at 1 μs pulse width. This results indicates that below 0.5 kV/cm, the ionic imbalance caused by the field can be handled easily by the

organism's ion balancing mechanisms, e.g., the sodium potassium pump. On the other hand, above 20 kV/cm the field ruptures the cell membrane and causes high ionic imbalance so that it is not possible for the hydrozoan's natural mechanisms to regain its balance. Between these values, the species needs to exert more energy to counterbalance the field effect. Optimum pulse width was shown to be in the sub-microsecond range, which means that pulse power is the most efficient tool to affect these macroscopic organisms. It was also concluded that it was a combination of field strength and the energy expenditure that determines the resultant stress. Therefore, it is not merely charging a capacitor to a certain level which stresses the organism. The organism's natural defense mechanisms play an important role in this process. Rectangular pulses had stronger effects than sine wave pulses in laboratory experiments on hydrozoans. This means that high frequency components are more effective, in agreement with the capacitive nature of the cell membranes. Repetition rate played a key role in obtaining cumulative effects. Above 20 Hz, the recovery process was not completed when the next pulse was applied, consequently, stronger effects could be obtained with the same energy expenditure. Consequently, the temporal range of the recovery process lies in the millisecond range. No more gain was obtained at higher frequencies, up to 50 kHz. This conforms to the concept of a refractory period in which the tissues do not respond to any external stimulus. To stun aquatic nuisance species for longer than 10 minutes, the assumed residence time for marine cooling systems, an electrical field of 5 kV/cm at pulse width of 1 μs was required. This result suggests that current semiconductor

technology can not provide simple pulsers for biofouling control; rather, gas tube or magnetic switch pulsers should be used in field systems.

Field experiments showed that the electric field can provide an effective, environmentally friendly, and inexpensive control method to the biofouling problem. In salt water of resistivity 50 Ω.cm, a field strength of 6.45 kV/cm at 770 ns provided 100% biofouling prevention. This result allowed us to estimate the cost of biofouling prevention in tidal water cooling systems having 10 minute residence time to be 1560 Gal/kWh. In other words, the cost of electrical energy is on the order of 10 cents for the treatment of 1560 gallons of tidal water. Analytical methods (eq. 4) indicate that the amount of water treated per unit energy increases by a factor of forty in fresh water having resistivity of 2000 Ω.cm. However, modeling studies, where the biological cell was described in terms of electrical components, indicate that the absolute gain is smaller, more on the order of five [22]. It should be possible to treat approximately 2100 gallons of fresh water with an energy of one kWh, at cost of 10 cents, and obtain results comparable to those obtained in tidal water with field of 6.45 kV/cm; i.e., a 100 % reduction in biofouling.

The most conclusive information, to date, obtained from the fresh water trial is related to scaling. Scaling was reduced and probably eliminated from forming on the electrodes, presumably because of the alternating polarity system used. This is a very important finding, since without a solution to the scaling problem the inexpensive, high-voltage, pulse-power mussel control systems would be impractical to operate. This study indicated the problem can be solved.

The settlement data is promising, in that it appeared to provide a high efficiency in reducing settlement, but the data were confounded. It is anticipated that the Megapulse system, which received a new megatron, will provide the positive and negative spikes in the continuation of the study, that veliger behavior/mortality data can be obtained during the next site visit, and that veliger settlement densities will be much higher when PVC plates are retrieved in the summer of 1998.

REFERENCES

1) J. Malmivuo, R. Plonsey, *Bioelectromagnetism*. New York: Oxford University Press, 1995.

2) P. Schwan, "Dielectric Properties of tissues," *in Handbook of Biological Effects of Electromagnetic Fields*, C. Polk and E. Postow, Eds. New York: CRC Press, 1996.

3) U. Zimmermann, G. Neil, *Electromanipulation of Cells*. New York: CRC Press, 1996.

4) D. Durand, "Electric stimulation of excitable tissue," in *The Biomedical Engineering Handbook*, J. Bronzino, Ed. New York: IEEE Press, 1995.

5) J. Christopher, "Aquatic nuisance species: Nature, transport, and regulation," in *Zebra Mussels and Aquatic Nuisance Species*, F. D'Itri, Ed. Michigan: Ann Arbor, 1997.

6) H. Woods, *Marine Fouling and Its Prevention*. Massachusetts: George Banta, 1967.

7) A. Burnett, *Biology of Hydra*. New York: Academic Press, 1973.

8) P. Tardent, and C. Weber, "A qualitative and quantitative inventory of nervous cells in hydra," in *Coelenterate Ecology and Behavior*, G. Mackie, Ed. New York: Plenum, 1976.

9) G. N. Glasoe and J. V. Lebacqz, *Pulse Generators*. New York: McGraw-Hill, 1948.

10) J. Bridges, and M. Preache, "Biological influences of power frequency electric fields: A tutorial review from a physical and experimental viewpoint," *Proc. IEEE*, vol. 69, pp. 1092-1120, Sept. 1981.

11) H. Jenner, and J. Mommen, "Control of zebra mussel in power plants and industrial settings," Proc. *2nd Internl. Zebra Mussel Conf.*, pp. 235-242, June 1989.

12) G. Smythe, C. Lange, J. Doyle, J. Moesch, and P. Sawyko, "Pulse power generated electric fields as a means to control zebra mussels," Proc. *5th Internl. Zebra Mussel and Other Aquatic Nuisance Species Conf.*, pp. 431-446, March 1995.

13) G. Pilwat, and U. Zimmermann, "Erythrocyte and ghost cytoplasmic resistivity and voltage dependent apparent size," *Biophys. J.*, vol. 44, pp. 397-403, Dec. 1983.

14) M. Kirpichenko, V. Mikheev, and E. Shtern, "Action of Electric Current on Dreissena Polymorpha Larvae and Planktonic Crustanceans with Short Exposures," Akad. Nauk., Moscow, SSSR, p. 76, Sept. 1963.

15) B. Ehrenberg, D. Farkas, E. Fluhler, Z. Lojewska, and L. Loew, "Membrane potential induced by external electric field pulses can be followed with a potentiometeric dye," *Biophys. J.*, vol. 51, pp. 833-837, May 1987.

16) D. Gaylor, "Physical mechanisms of cellular injury in electrical trauma," Ph.D. dissertation, Massachusetts Insist. Tech. , 165 p., 1989.

17) M. Rader, S. Levy, I. Alexeff, A. Drake, J. Johnson, "The use of pulse power to control zebra mussel," Proc. *3rd Internl. Zebra Mussel Conf.*, pp. 173-192, March 1993.

18) D. Gross, M. Loew, and W. Webb, "Optical imaging of cell membrane potential changes induced by applied electric fields," *Biophys. J.*, vol. 50, pp. 339-348, August 1986.

19) S. Cole, "Electric impedance of marine egg membranes," *Trans. Faraday Soc.*, vol. 23, pp. 966-972, March 1937.

20) K. Schoenbach, A. Abou-Ghazala, T. Vithoulkas, R. Alden, R. Turner, S. Beebe, "The effect of pulsed electrical fields on biological cells", Proc. *11th IEEE International Pulsed power Conf.*, pp. 504-509, June 1997.

21) G. Smythe, J. Doyle, T. Reed, and P. Sawyko, "Application of cost effective electric fields to deter attachment of the zebra mussel to structures," Proc. *4th Intrl. Zebra Mussel Conf.*, Madison, WI, pp. 335-350, April 1994.

22) J. Hudgins, "A review of modern power semiconductor devices," *Microelec. J.*, vol. 24, pp. 41-54, Jan. 1993.

23) H. Schwan, K. Foster, "RF-Field interaction with biological systems: Electrical properties and biophysical mechanisms", *Proc. IEEE*, vol. 68, pp. 104-113, Jan. 1980.

24) J. Baggs, US Pat. 2295, Sept. 1863.

25) G. Dellius, and C. Tarto, US Pat. 1021734, March 1912.

26) J. Wilkie, US Pat. 1467890, Sept 1923.

27) G. Cox, US pat. 2200469, 1940.

28) K. Schoenbach, A. Abou-Ghazala, R. Alden, T. Turner, T. Fox, "Biofouling prevention with pulsed electric fields", Proc. *7th International Zebra Mussel and Aquatic Nuisance Species Conf.*, pp. 309-313, Jan 97.

29) G. Smythe, K. Schoenbach, C. Lange, A. Abou-Ghazala, "Pulse power electric fields as a method to prevent settlement and/or Induce Mortality in Zebra Mussels", Proc. *8th International Zebra Mussel and Aquatic Nuisance Species Conf.*, pp. 406-411, March 98.

APPENDIX A

PULSE POWER SYSTEMS FOR THE MICROSECOND AND SUB-MICROSECOND TEMPORAL RANGE

A.1 Introduction

Pulse power is the generation of very short duration pulses, up to microsecond range, with long inter pulse duration. The shape of the pulse is usually rectangular with voltage magnitude up to megavolts. Due to the short duration of the pulses, the power of the pulse can be made very high, up to terawatt, with practical energy expenditure. Applications of pulse power are numerous, ranging from biofouling control to medical applications. Some typical applications for microsecond and sub-microsecond pulse generators are microwave radar, laser diode drive circuits, sweep circuits for CRT streak cameras, the gating of micro-channel plates, triggering of scopes and transient recorders. In this appendix, pulse power generator types will be introduced and analyzed with emphasize on the types suitable for our application of biofouling control.

A.2 The Basic Circuit of a Pulse Generator

The pulse generators depend on the storage of electrical energy either in an electrostatic field or in a magnetic field, and the subsequent discharge of a fraction or all of this stored energy into the load. The two basic categories into which the largest number of pulser designs fall are: 1) those in which only a small fraction of the stored energy is discharged into the load during a pulse (hard tube pulsers), and 2) those in which all of the stored energy is discharged each pulse

(line type pulsers). Line type pulsers are divided again into current fed pulsers, and voltage fed pulsers. To accomplish the discharge, it is necessary to provide a suitable switch that can be closed (or open) for a length of time corresponding to the pulse duration and maintain the other case for a time corresponding to build up the stored energy again before the next succeeding pulse. The characteristic required for the switch would be different depending on whether or not all the stored energy is discharged into the load during a single pulse. Some pulse shaping will be necessary in the discharging circuit when all the energy is to be dissipated. The basic schematic diagram for a pulse generator is shown in figure A.1.

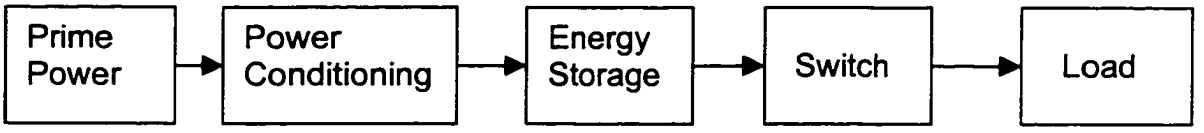

Fig. A.1. Basic schematic diagram of pulse generators

A.3 Pulse Generator Types

A.3.1 Hard tube pulsers

In general, the energy storage device for these pulsers is simply a condenser that is charged to some voltage V, thus making available an amount of electrical energy $CV^2/2$. The switch controls the small fraction of energy released the load by closing and opening at the appropriate times. The voltage across the switch immediately after the pulse and during the charging interval is nearly the same as it is at the beginning of the pulse, this requires special closing

and opening characteristics for the switch. A fast power supply is usually used to charge the capacitor between pulses. An isolating element is introduced in the charging circuit to isolate the charging circuit from the discharging circuit in the discharge mode. This element may be a high resistance or an inductance depending on the overall pulser design. The impedance of this isolating element should not be so high that the voltage on the condenser at the end of the interpulse interval differs appreciably from the power supply voltage. For nanosecond pulsers, high speed density capacitors should be used and they are commercially available. Switch selection varies from semiconductor switches to gas tube switches, depending on the voltage and current rating required and the required conduction characteristics. This will be discussed in the switch analysis part. Schematic diagram for the hard tube pulser is shown in figure A.2 [9].

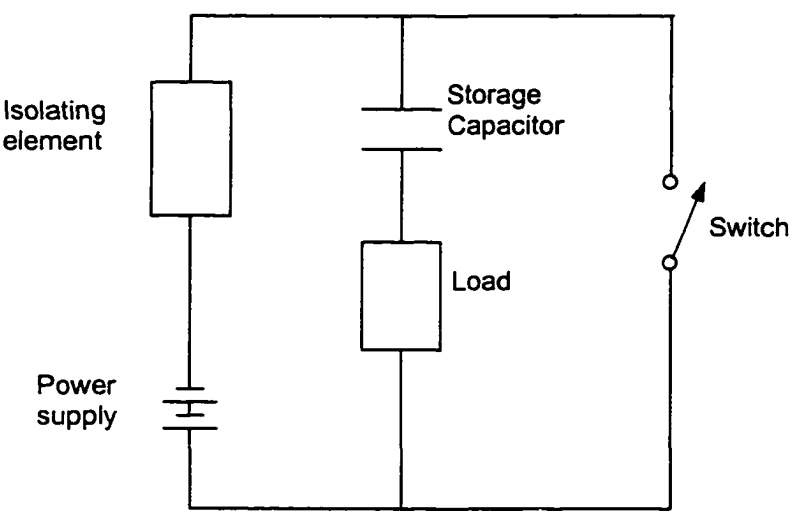

Fig. A.2. Hard tube pulse generator circuit

A.3.2 Line type pulsers

Pulse generators in this category are referred to as "line type" pulsers because the energy storage device is essentially a lumped constant transmission line. Since this component of the line type pulser serves not only as the source of electrical energy during the pulse but also as the pulse shaping element, it has commonly known as a "pulse forming network", PFN. There are essentially two classes of pulse forming networks, those in which the energy for the pulse is stored in an electrostatic field in the amount 0.5 CV^2, and those in which this energy is stored in magnetic field in the amount 0.5 LI^2. The first class is referred to as "voltage fed networks" and the second as "current fed network." For most applications, the voltage fed network has been used extensively, i.e., in the microwave radar applications, in preference to the current fed networks because of the lack of satisfactory switch tubes for the latter type. However, the introduce of the new semiconductor high ratings opening switch may open the door to current fed network applications, especially that this kind has much higher energy density (25 times) than the voltage fed type. The pulse forming network in a line type pulser consists of inductances and condensers which may be put together in many possible configurations. The configuration chosen for a particular purpose depends on the ease with which the network can be fabricated, as well as on the specific pulser characteristics required. This category includes voltage fed pulsers and current fed pulsers.

The consideration of impedance matching is of extreme importance in designing a line type pulsar because it affects the utilization of the energy stored

in the network, as well as the ultimate shape of the voltage and current pulses at the load. For these reasons, the nature of the load must be known before proceeding to the design of the pulser.

A.3.2.1 voltage fed line type pulsers

A schematic diagram is shown in figure A.3 for the circuit of voltage fed pulser.

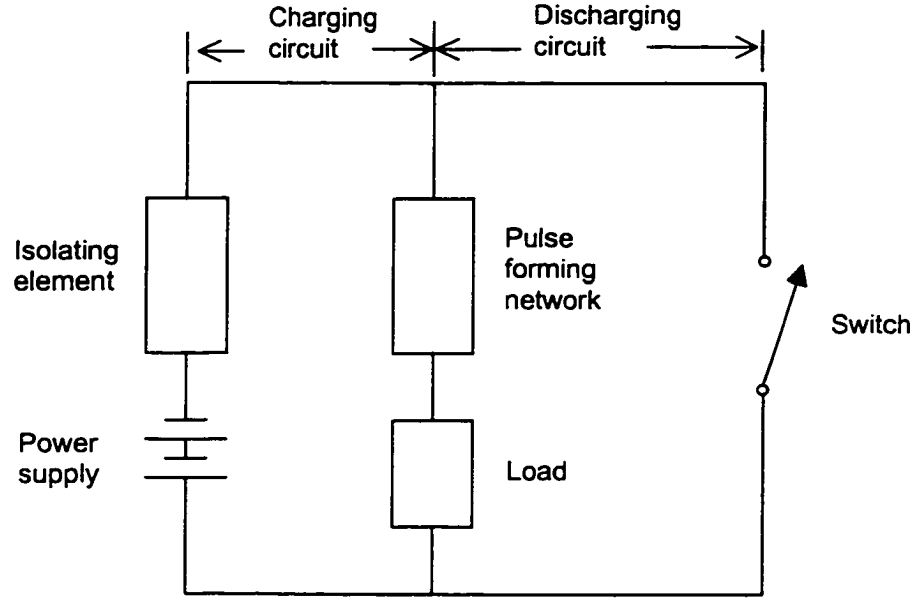

Fig. A.3. Charging and discharging circuit for a voltage fed line type pulser

Charging the pulse forming network (PFN) from the power supply is completed first when the switch is open. Closing the switch will allow the discharge of the energy into the load. When the load impedance is equal to the characteristic impedance of the network, assuming the switch to have a negligible resistance, all of the energy stored in the network is transferred to the load, leaving the condensers in the network completely discharged. The time required for this energy transfer determines the pulse duration and depends on

the values of the capacitances and inductances of the network. If the load impedance is not equal to the network impedance, reflections at the load will happen and the pulse shape will no longer be square. Switch performance is crucial to the performance. Switches analysis and selection criteria will be discussed later in this chapter.

A.3.2.2 Current fed line type pulsers

Figure A.4 shows a schematic diagram for the current fed pulsers.

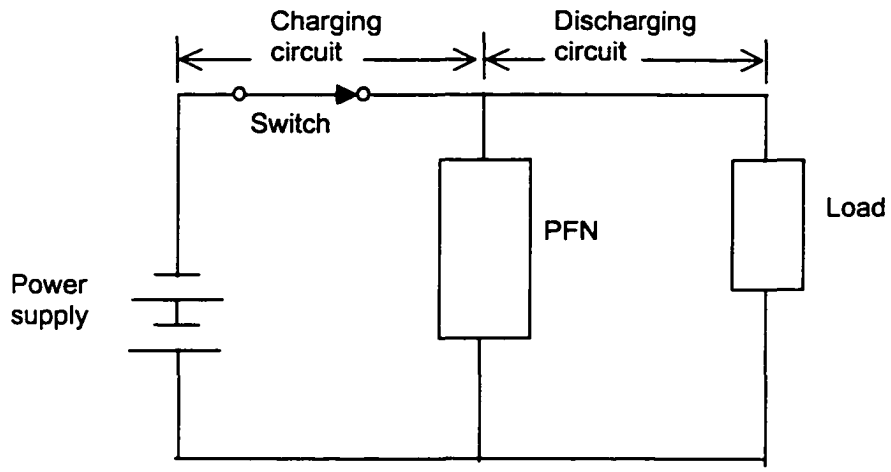

Fig. A.4. Charging and discharging circuit for a current fed pulser

In this type, the switch acts to close the network charging circuit and allows a current to build up in the inductance of the network. When this current is interrupted by opening the switch, a high voltage, whose magnitude depends on the load impedance and the current in the inductance, appears across the load. Energy density stored in the magnetic field is much higher than electric field, around 25 joule per cubic centimeter, but the main difficulty in wide usage of this pulser is finding a durable long life switch. Plasma opening switch and opening

switches based on the electric explosion of wires were used, but such opening switches can not operate repetitively, or have a restricted lifetime because of electrode erosion. However, there is a new semiconductor opening switch, which may open the door to the existence of reliable current fed pulsers.

A.4 Pulse Power Switching Devices

The switch is the heart of any pulse power generator. Switch ratings, rise time, fall time, and triggering requirements are what actually determine the pulser performance. Switching devices that meet high, stringent requirements often require specialized technologies or skills to manufacture. For microsecond and sub-microsecond temporal range, gaseous tube switches, semiconductor switches, laser triggered spark gap switch, and optically controlled switches are the different choices for the closing switch, the new semiconductor opening switch is the candidate as opening switch. Each of these choices will be discussed below.

A.4.1 Gaseous tube switches

Thyratron: Arc discharge and plasma formation is the basic idea. Different gases can be used for filling these devices depending on the characteristic required. Very high voltage blocking capabilities (up to 100 kV), and current ratings (up to 10 kA) can be achieved. Switching time can be as low as 20 nsec for lower rates. Switching requirements are 700 to 1000 V triggering pulse. Also heating the tube is required. Life time is around 10^9 shots. Cost and relatively short life (3 years at 10 Hz) are the major disadvantages.

Spudo Spark: This is a gas filled tube with two electrodes to establish the discharge between them according to the left of Pachon curve. High blocking voltage (up to 50 kV) and high conduction currents (up to 100 kA) are achievable. Typical life time is around 10^8 shots. The major advantage is that it can withstand oscillation. Disadvantages are the electrode erosion and short life span.

Krytron: Krytrons are a highly specialized variety of cold cathode trigger tube. The krytron is designed to switch moderately high impulse currents (up to 3 kA) and voltages (up to 5 kV) in an arc discharge mode. It is able to turn on this arc very rapidly as it relies on an already present plasma to support the conduction, rather than waiting for the plasma to be formed. Commutation times below 1 nsec are achievable with krytrons. It requires a high voltage pulse (500V to 2 kV) to be applied to the trigger electrode to fire successfully. Short life (as few as 200 shots) is a major disadvantage for repetitive applications.

A.4.2 Laser triggered spark gap

The spark gap is essentially just two electrodes with a gap in between. When the voltage between the electrodes exceeds the breakdown voltage of the gas, the device arcs and a current is established very rapidly. Laser triggering for spark gaps is the fastest way to form a plasma and establish the conduction in about 10 nsec. Very high voltage ratings (>100 kV) and current ratings (>10 kA) are obtainable. Short life time due to electrode erosion and the need for the laser are the major disadvantages.

A.4.3 Solid state switches

The basic limitations to semiconductor closing switches are the current and voltage ratings. This problem may be decreases with the nanosecond pulses as the power ratings decrease. There are now a few commercially available transistors on the market that can handle few kV and few hundreds of pulsed currents in sub-nanosecond temporal range. But above this range other choices are a must. Switching speed and trigger requirements are another important consideration. Table A.1 summarizes the ratings and the characteristics of these switches [22].

Table A.I
Ratings and characteristics of different semiconductor switches

	Thyristors	GTOs	Power MOSFETs	IGPTs	MCTs
Manufacturer	AEG, ASEA, GE, Motorola, Siemens, ..	AEG, BBC, Powerex, Philips, Toshiba, ..	GE, Harris Motorola, Powerex, Siemens, ..	GE, Ixys, Motorola, Toshiba, Siemens	GE, Siemens, Harris, Toshiba
Major Applications	Very high power switchgear, DC HV transmission	Locomotive drives, UPS, Pumps	Switching power supplies, motor drives, RF generators	Motor drives, power supplies	Motor control, inverters, line switches
Max forward Blocking Volt (V)	8000	5000	1500	1200	3000
Max current (A)	5000	3000	100	100	100
Max frequency (kHz)	50	20	25000	50	50
Max dv/dt (V/μs)	600	1500	200000	100000	50000
Max dI/dt (A/μs)	1200	300	30000	5000	4000
Max operating Temp (°C)	125	125	200	200	150
Switching Requirements	Needs external commutation, or ac voltage to turn off	Small gate ct for turn on, very large gate ct to turn off	Very low gate ct for turn on, or turn off	Very low gate ct for turn on or turn off	Very low negative pulse for turn on, small positive ct for Turn off

IMAGE EVALUATION TEST TARGET (QA-3)

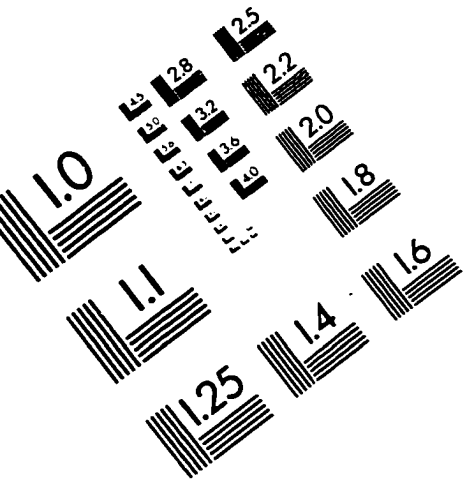

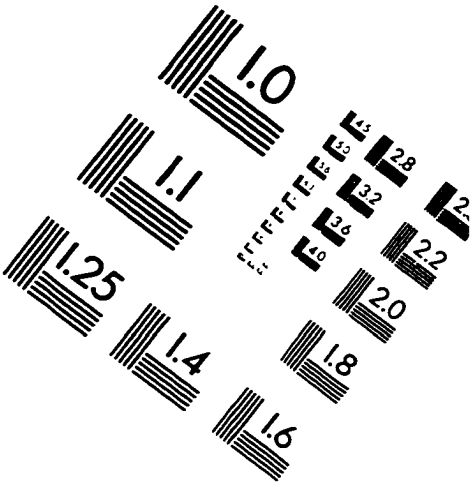

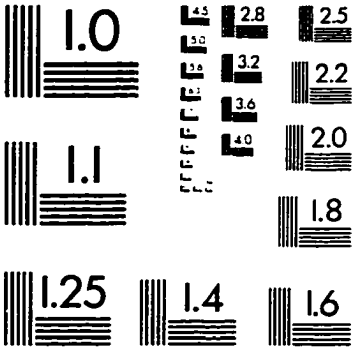

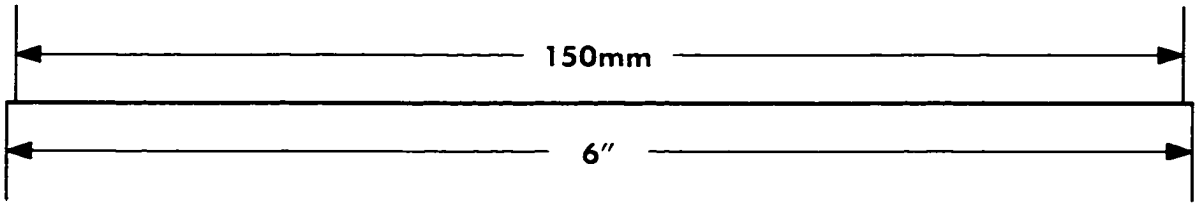

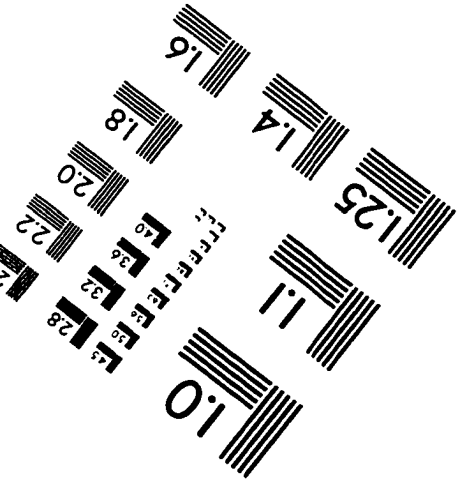

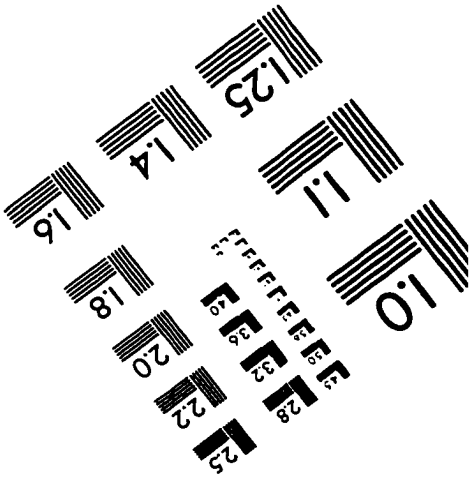

APPLIED IMAGE, Inc
1653 East Main Street
Rochester, NY 14609 USA
Phone: 716/482-0300
Fax: 716/288-5989